International Standard

ISO/IEC 29794-4

Information technology — Biometric sample quality —

Part 4:
Finger image data

Technologies de l'information — Qualité d'échantillon biométrique —

Partie 4: Données d'image de doigt

Second edition
2024-09

Contents

Page

Foreword

ISO (the International Organization for Standardization) and IEC (the International Electrotechnical Commission) form the specialized system for worldwide standardization. National bodies that are members of ISO or IEC participate in the development of International Standards through technical committees established by the respective organization to deal with particular fields of technical activity. ISO and IEC technical committees collaborate in fields of mutual interest. Other international organizations, governmental and non-governmental, in liaison with ISO and IEC, also take part in the work.

The procedures used to develop this document and those intended for its further maintenance are described in the ISO/IEC Directives, Part 1. In particular, the different approval criteria needed for the different types of document should be noted. This document was drafted in accordance with the editorial rules of the ISO/IEC Directives, Part 2 (see www.iso.org/directives or www.iec.ch/members_experts/refdocs).

ISO and IEC draw attention to the possibility that the implementation of this document may involve the use of (a) patent(s). ISO and IEC take no position concerning the evidence, validity or applicability of any claimed patent rights in respect thereof. As of the date of publication of this document, ISO and IEC had not received notice of (a) patent(s) which may be required to implement this document. However, implementers are cautioned that this may not represent the latest information, which may be obtained from the patent database available at www.iso.org/patents and https://patents.iec.ch. ISO and IEC shall not be held responsible for identifying any or all such patent rights.

Any trade name used in this document is information given for the convenience of users and does not constitute an endorsement.

For an explanation of the voluntary nature of standards, the meaning of ISO specific terms and expressions related to conformity assessment, as well as information about ISO's adherence to the World Trade Organization (WTO) principles in the Technical Barriers to Trade (TBT) see www.iso.org/iso/foreword.html. In the IEC, see www.iec.ch/understanding-standards.

This document was prepared by Joint Technical Committee ISO/IEC JTC 1, *Information technology*, Subcommittee SC 37, *Biometrics*.

This second edition cancels and replaces the first edition (ISO/IEC 29794-4:2017), which has been technically revised.

The main changes are as follows:

— algorithms for normalization of finger image quality components have been added, along with new quality algorithm identifiers for the unique identification of the quality measures defined in this document;

— Annex A has been technically revised to reflect a new conformance test set.

A list of all parts in the ISO/IEC 29794 series can be found on the ISO and IEC websites.

Any feedback or questions on this document should be directed to the user's national standards body. A complete listing of these bodies can be found at www.iso.org/members.html and www.iec.ch/national-committees.

Introduction

This document specifies finger image quality measures. A reference implementation of the normative measures — NFIQ 2 — is available at Reference [16], which is described in more detail by the developers in Reference [1].

The quality of finger image data is determined by the degree to which the finger image data fulfils specified requirements for the targeted application. Information on quality is therefore useful in many applications. ISO/IEC 19784-1 allocates a quality field and specifies the allowable range for the scores, with a recommendation that the score be divided into four categories with a qualitative interpretation for each category. Finger image quality fields are provided in the finger image data interchange formats standardized in ISO/IEC 19794-4 and ISO/IEC 39794-4. Finger feature data interchange formats standardized in ISO/IEC 19794-2, ISO/IEC 19794-3, ISO/IEC 19794-8 and ISO/IEC 39794-2 provide finger image quality fields for the source image. To facilitate the interpretation and interchange of finger image quality scores, this document specifies how to calculate the finger image quality score of plain finger images with a spatial sampling rate of 196,85 px/cm and a bit depth of 8 bit for the greyscale pixel intensity values scanned from inked fingerprint cards or captured using optical area sensors based on frustrated total internal reflection.

Information technology — Biometric sample quality —

Part 4:
Finger image data

1 Scope

This document establishes:

— terms and definitions for quantifying finger image quality;

— methods used to quantify the quality of finger images; and

— standardized encoding of finger image quality;

for finger images at 196,85 px/cm spatial sampling rate and a bit depth of 8 bit for the greyscale pixel intensity values scanned or captured using optical area sensors in direct contact with friction ridges.

2 Normative references

The following documents are referred to in the text in such a way that some or all of their content constitutes requirements of this document. For dated references, only the edition cited applies. For undated references, the latest edition of the referenced document (including any amendments) applies.

ISO/IEC 2382-37, *Information technology — Vocabulary — Part 37: Biometrics*

ISO/IEC 39794-1, *Information technology — Extensible biometric data interchange formats — Part 1: Framework*

ISO/IEC 29794-1, *Information technology — Biometric sample quality — Part 1: Framework*

3 Terms and definitions

For the purposes of this document, the terms and definitions given in ISO/IEC 2382-37, ISO/IEC 29794-1 and the following apply.

ISO and IEC maintain terminology databases for use in standardization at the following addresses:

— ISO Online browsing platform: available at https://www.iso.org/obp

— IEC Electropedia: available at https://www.electropedia.org/

3.1
foreground region
set of all pixels of a finger image that form valid finger image patterns

Note 1 to entry: The most evident structural characteristic of a valid finger image is a pattern of interleaved ridges and valleys.

3.2
local region
block of $m \times n$ pixels of the foreground region, where m and n are smaller than or equal to the width and the height of the foreground region respectively

3.3
finger image quality assessment algorithm
algorithm to calculate a quality measure

Note 1 to entry: "Quality assessment algorithm" and "quality algorithm" are synonyms.

3.4
trim
removal of pixels from the top, left, bottom and right sides of a finger image that do not comprise the foreground region

Note 1 to entry: The steps for trimming an image to form the foreground region are defined in 6.1.5.2.

4   Abbreviated terms

CBEFF   Common Biometric Exchange File Format

DFT   discrete Fourier transform

DT   determine threshold

FDA   frequency domain analysis

FJFX   FingerJet Fingerprint Feature Extractor, Open Source Edition

LCL   local clarity

NFIQ   NIST Fingerprint Image Quality

OCL   orientation certainty level

OFL   orientation flow

QSND   quality score normalisation dataset

RVU   ridge valley uniformity

TIR   total internal reflection

5   Conformance

A finger image quality assessment algorithm conforms to this document if it conforms to the normative requirements of Clause 6.

A finger image quality block shall conform to this document if its structure and data values conform to the formatting requirements of Clause 7 (finger image quality block) and if its quality values are computed using the methods specified in 6.2 and 6.4.

A finger image quality assessment implementation conformant to this document may use the biometric organization identifier of ISO/IEC JTC 1/SC 37, which is 257 (101_{Hex}), if it has been tested following the conformance testing methodology in Clause A.2.

Conformance to normative requirements of Clause 7 is achieved by Level 1 and Level 2 conformance as specified in ISO/IEC 39794-1:2019, Annex C. Conformance to normative requirements of 6.2 and 6.4 is achieved by Level 3 conformance as specified in ISO/IEC 39794-1:2019, Annex C.

The conformance test assertion in Annex A shall apply.

6 Finger image quality measures

6.1 Overview

6.1.1 General

This clause establishes measures for predicting the utility of a finger image. Image quality measures from a single image are useful to ensure the acquired image is suitable for recognition.

A complete finger image quality analysis shall examine both the local and global structures of the finger image. Fingerprint local structure constitutes the main texture-like pattern of ridges and valleys within a local region while valid global structure puts the ridges and valleys into a smooth flow for the entire fingerprint. The quality of a finger image is determined by both its local and global structures. This clause describes the features and characteristics of finger images at both local and global structures that are to be used as quality components for quantifying finger image quality.

For applying the algorithms as described in 6.2 and 6.3, the finger image shall have a spatial sampling rate of 196,85 pixels per centimetre (500 pixels per inch), a bit depth of 8 bit for the greyscale pixel intensity values, with friction ridges represented by greyscale pixel intensity values lower than those for valleys. The algorithms were developed using images of finger friction ridges in contact with an electronic capture device and inked fingerprints digitized with an electronic scanner. The imaging devices and scanners are considered free from geometric distortion and exhibit greyscale linearity and uniformity.

ISO/IEC 29794-1 requires that quality components be mapped to an integer value between 0 and 100, inclusive.

6.1.2 Methods for mapping to the desired value range

6.1.2.1 Sigmoid function

The mapping of values between 0 and 1 inclusive is accomplished for several quality components with the sigmoid function as shown in Formula (1):

$$\text{sigmoid}(x, x_0, w) = \left(1 + \exp\left(\frac{x_0 - x}{w}\right)\right)^{-1} \tag{1}$$

where

x is a native quality measure value;

x_0 is the inflection point at which the function has the value 0,5;

w is a scaling parameter determining the width of the region in which the function transitions from ε to $1-\varepsilon$;

ε is an infinitesimally small positive quantity.

The values computed from the sigmoid function will be mapped to the target value ranges (0 to 100) in subsequent clauses.

6.1.2.2 Known ranges

When the range of values for a given quality measure is known (e.g. from 1 to 250, inclusive), the known range function is used, as shown in Formula (2):

$$\left\lfloor \frac{x - \min(x)}{\max(x) - \min(x) + \varepsilon} 101 \right\rfloor \tag{2}$$

where

x is a native quality measure value;

$\lfloor x \rfloor$ is the floor function giving the greatest integer $\leq x$

ε is an infinitesimally small positive quantity.

6.1.3   Constituent of local quality measures

A finger image is partitioned into local regions such that each local region contains sufficient ridge-valley information, preferably having at least two clear ridges, while not overly constraining high curvature ridges. For images with a spatial sampling rate of 196,85 pixels per centimetre (500 pixels per inch), the ridge separation usually varies between 8 pixels to 12 pixels.[2] A ridge separation comprises a ridge and a valley. In order to cover two clear ridges, the local region size has to be greater than 24 pixels in both width and height. The size for each local region shall be (32 × 32) pixels, which is sufficient to cover two clear ridges. Instead of Cartesian coordinate, curvilinear coordinate along the ridge can also be used.

NOTE   The size of the local region used during computation of q_{OFL}^{σ} (6.2.16.3), q_{OFL}^{μ} (6.2.16.2), $q_{\text{COH}}^{\text{sum}}$ (6.2.14), and $q_{\text{COH}}^{\text{rel}}$ (6.2.15) in the reference implementation NFIQ 2 prior to version 2.3.0 deviates from size specified in this subclause.

6.1.4   Constituent of global quality measures

A global quality measure shall be computed over the whole finger image after trim to assess the utility of the sample for fingerprint recognition.

6.1.5   Image preprocessing

6.1.5.1   Description

A segmentation process follows where each local region is labelled as background or foreground. There are several segmentation approaches, such as using the average magnitude of the pixel-intensity gradient in each local region.[2]

This document does not prescribe segmentation methods, but notes that performing segmentation influences several quality components. Constant or near constant areas of the input image shall be removed according to 6.1.5.2 prior to computing quality using the measures specified in 6.2 and 6.3.

See Annex C for the area consideration.

6.1.5.2   Removal of near constant rows and columns in image

Prior to computing quality components, fingerprint images shall be trimmed to remove near constant rows and columns on the margins. Pixel intensities take values [0, 255] for an 8-bit greyscale image. As a first approximation of the region of interest, image columns and rows which are near constant white background are removed. Using the algorithm specified below, a fixed threshold, T_{μ}, is set to the greyscale pixel intensity of 250 to obtain the image without near constant areas.

The algorithm is visualized in Figure 1 and specified as follows:

a)   For each row R_i in $\hat{I}$, starting from the top:

   1)   compute the row arithmetic mean μ_{row};

   2)   on the first occurrence where $\mu_{\text{row}} \leq T_{\mu}$ set $\text{top} = R_i$;

3) on the last occurrence where $\mu_{\text{row}} \leq T_\mu$ set $\text{bottom} = R_i$.

b) For each column C_i in $\hat{I}$, starting from the left:

1) compute the column arithmetic mean μ_{col};

2) on the first occurrence where $\mu_{\text{col}} \leq T_\mu$ set $\text{left} = C_i$;

3) on the last occurrence where $\mu_{\text{col}} \leq T_\mu$ set $\text{right} = C_i$.

c) extract the trimmed region of interest, I, as the pixels of $\hat{I}$ encompassed between and including the rows top (a2) and bottom (a3) and the columns left (b2) and right (b3).

where

$\hat{I}$ is the matrix of grey levels corresponding to the pixels of an image;

I is the matrix of grey levels corresponding to the pixels of an image after trim.
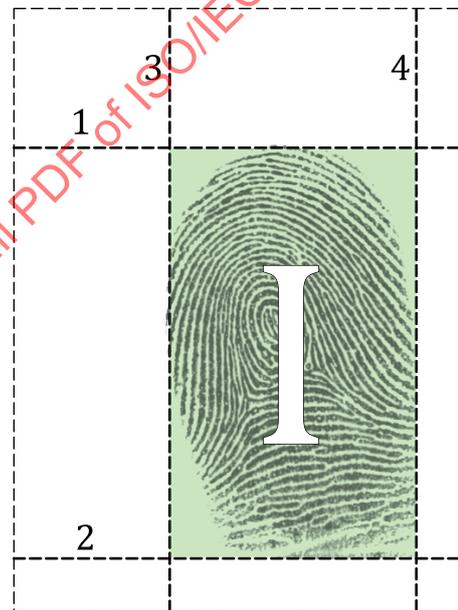
a) Image prior to trimming near constant rows and columns on the margins

b) Results of following the steps in 6.1.5.2

Key

1   top

2   bottom

3   left

4   right

NOTE 1   In Figure 1 a), the area overlayed in green is a visualisation of $\hat{I}$.

NOTE 2   In Figure 1 b), the area overlayed in green is a visualisation of I.

NOTE 3   Each subfigure within Figure 1 contains a dashed black border.

Figure 1 — Example of removing near constant white rows and columns from an image

6.1.5.3 Foreground segmentation based on local standard deviation

For quality components that require a foreground mask to indicate regions containing the fingerprint, an algorithm using local standard deviation is adopted.

The algorithm is specified as follows:

a) Normalize I to zero mean and unit standard deviation to produce I'.

b) For each local region V in I':

    1) compute the standard deviation of V as σ_v ;

    2) mark the corresponding local region in I_{mask} as foreground if $\sigma_v > 0,1$.

6.1.5.4 Computing the dominant ridge flow orientation for a local region from pixel-intensity gradients

The dominant ridge flow orientation is determined by computing the pixel-intensity gradient information and then determining the orientation of the principal variation axis.

The numerical gradient of the local region is determined using finite central difference for all interior pixels in x-direction and y-direction, as shown in Formulae (3) and (4):

$$f_x = \frac{I(x+1,y) - I(x-1,y)}{2} \tag{3}$$

$$f_y = \frac{I(x,y+1) - I(x,y-1)}{2} \tag{4}$$

With f_x and f_y, the dominant ridge flow orientation, angle(V), is determined analytically using the sine and cosine doubled angle determined from the arithmetic means of the pixel-intensity gradient covariances, as shown in Formulae (5) to (12):

$$a = \overline{f_x^2} \tag{5}$$

$$b = \overline{f_y^2} \tag{6}$$

$$c = \overline{f_x f_y} \tag{7}$$

$$C = \begin{bmatrix} a & c \\ c & b \end{bmatrix} \tag{8}$$

$$d = \sqrt{c^2 + (a-b)^2} \tag{9}$$

$$\sin(\theta) = \frac{c}{d} \tag{10}$$

$$\cos(\theta) = \frac{a-b}{d} \tag{11}$$

$$\text{angle}(V) = \frac{1}{2}\arctan\left(\frac{\sin(\theta)}{\cos(\theta)}\right) \tag{12}$$

NOTE   In Formulae (5), (6) and (7), the use of the overbar indicates the mean of the value.

6.1.6 Image examples

For algorithms operating in a block-wise manner the trimmed input image is subdivided into local regions according to an overlay grid. This is demonstrated in Figure 2 b), in which the local region V (6,1) is used as an example in local processing and is marked up using a bold blue line. Figure 2 c) shows an enlarged view of V (6,1) and Figure 2 d) shows V (6,1) rotated according to its dominant ridge orientation computed using Formula (12).

| a) Input finger image | b) Division into local regions | c) Enlarged view of V (6,1) | d) V (6,1) rotated according to its dominant ridge orientation as determined using Formula (12) |
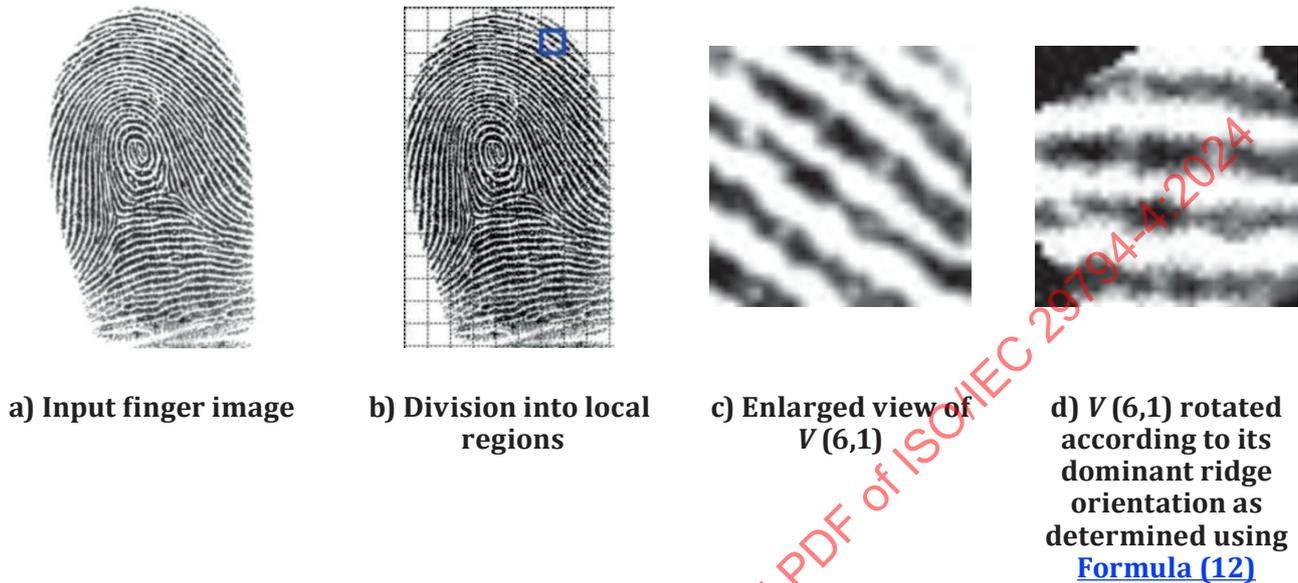
Figure 2 — Example of computing the dominant ridge flow orientation for a local region

6.2 Normative contributive quality components

6.2.1 General

Subclause 6.2 specifies algorithms for computing finger image quality components that contribute to the ISO/IEC 29794-4 quality feature vector and to the computation of the unified quality score.

6.2.2 Orientation certainty level

6.2.2.1 Description

The orientation certainty level (OCL)[3] of a local region is a measure of the consistency of the orientations of the ridges and valleys contained within this local region. The feature computes local quality and operates in a block-wise manner.

The finger image within a (32 × 32) pixels local region [as shown in Figure 2 c)] generally consists of dark ridge lines separated by white valley lines along the same orientation. The consistent ridge orientation and the appropriate ridge and valley structure are distinguishable local characteristics of the fingerprint local region.

The pixel-intensity gradient (dx, dy) at a pixel describes the direction of the maximum pixel-intensity change and its strength. By performing principal component analysis on the pixel-intensity gradients in a local region, an orthogonal basis for the local region can be formed by finding its eigenvalues and eigenvectors. The resultant first principal component contains the largest variance contributed by the maximum total gradient change in the direction orthogonal to ridge orientation. The direction is given by the first eigenvector and the value of the variance corresponds to the first eigenvalue, λ_{max}. On the other hand, the resultant second principal component has the minimum change of gradient in the direction of ridge flow which corresponds to the second eigenvalue, λ_{min}. The ratio between the two eigenvalues thus gives an

indication of the strength of the energy concentrated along the dominant direction with two vectors pointing to the normal and tangential direction of the average ridge flow respectively.

6.2.2.2 Computing the eigenvalues and local orientation certainty

From the covariance matrix C [Formula (8)] the eigenvalues λ_{min} and λ_{max} are computed as shown in Formulae (13) and (14):

$$\lambda_{min} = \frac{a + b - \sqrt{(a-b)^2 + 4c^2}}{2} \tag{13}$$

$$\lambda_{max} = \frac{a + b + \sqrt{(a-b)^2 + 4c^2}}{2} \tag{14}$$

This yields the local orientation certainty level shown in Formula (15):

$$q_{OCL}^{local} = \begin{cases} 1 - \dfrac{\lambda_{min}}{\lambda_{max}}, & \text{if } \lambda_{max} > 0 \\[2mm] \qquad 0, & \text{otherwise.} \end{cases} \tag{15}$$

which is a ratio in the interval [0,1] where 1 is highest certainty level and 0 is lowest.

NOTE   The orientation certainty level fails to predict recognition performance when some marks or residue exist in the samples that have strong orientation strength, such as those exhibited by latent prints left by the previous user of a capture device.

6.2.2.3 OCL algorithm

For each local region V in I:

a)   compute the pixel-intensity gradient of V with the centred differences method [Formulae (3), (4)];

b)   compute the covariance matrix C [Formula (8)];

c)   compute the eigenvalues of C to obtain q_{OCL}^{local} [Formulae (13), (14), (15)].

Figure 3 visualizes the processing steps.

a) Current local region with the ratio between eigenvalues marked as ellipse
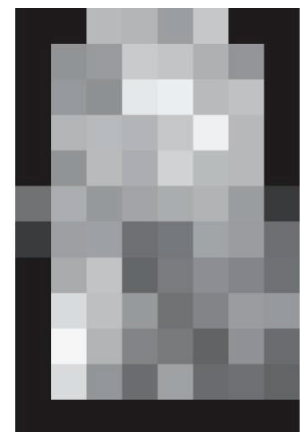
b) Original, untrimmed image and its q_{OCL}^{local} values, mapped to values 0-255

Figure 3 — Processing steps of orientation certainty level quality algorithm

6.2.3 Local clarity

6.2.3.1 Description

Good quality fingerprints exhibit clear ridge-valley structure. Thus, the local clarity (LCL),[4] which is the measure of the ridge-valley structure clarity, is a useful indicator of the quality of a fingerprint. The feature computes local quality and operates in a block-wise manner.

To perform ridge-valley structure analysis, the foreground of the finger image is quantized into local regions of size (32 × 32) pixels.[3] Inside each local region, an orientation line, which is perpendicular to the ridge direction, is computed. At the centre of the local region along the ridge direction, a local region of size (32 × 16) pixels shall be extracted and transformed to a vertically aligned local region.

A linear regression (or least square fitting) is applied to calculate the determine threshold (DT), which is a line positioned at the centre of the local region V used to segment the local region into the ridge and valley regions. Regions with grey levels lower than DT are classified as ridges. Otherwise, they are classified as valleys.

Since good finger images cannot have ridges that are too close or too far apart, the nominal ridge and valley thickness can be used as a measure of the quality of the finger image captured. Similarly, ridges that are unreasonably thick or thin indicate that the finger image has not been captured properly (due to pressing too hard or too softly, for example), or that the image is a residual sample. Thus, the finger image quality can be determined by comparing the ridge and valley thickness to each of their nominal range of values. Any value out of the nominal range can imply a bad quality ridge pattern. To normalize the range of the thickness values, a pre-set maximum thickness is used. The maximum ridge or valley thickness, W_{max}, for a good finger image is estimated at 20 pixels for a 196,85 pixels per centimetre (500 pixels per inch) scanner spatial sampling rate. The pre-set value of 20 pixels for a 196,85 pixels per centimetre (500 pixels per inch) scanner spatial sampling rate is obtained from the median of the typical ridge separation of (8 – 12) pixels,[2] and assuming that any ridge separation will not exceed twice the median value. This will ensure that the pre-set value is indeed the maximum to limit the value of the normalized ridge and valley thickness between 0 and 1. The ridge thickness, W_r, and valley thickness, W_v, are then normalized with respect to the maximum thickness, W_{max}.

With the ridge and valley separated as above, a clarity test can be performed in each segmented rectangular 2D region.

For local regions with good clarity, the pixel-intensity distribution of ridges and the pixel-intensity distribution of the valleys have a very small overlapping area and thus q_{LCL}^{local} is high. The following factors affect the size of the total overlapping area:

a) noise on ridge and valley;

b) water patches on the image due to wet fingers;

c) incorrect orientation angle due to the effect of directional noise;

d) scar across the ridge pattern;

e) highly curved ridges;

f) ridge endings, bifurcations, delta and core points;

g) incipient ridges, sweat pores, and dots.

Factors a) to c) are physical noise found in the image. Factors d) to g) are actual physical characteristics of the fingerprint. See Annex B for the factors influencing fingerprint image quality.

6.2.3.2 Computing the ridge valley signature of a local region

Given the local region **V**, the ridge valley signature **S** is obtained according to Formula (16):

$$S(x) = \frac{\sum_{y=1}^{16} V_{x,y}}{16} \tag{16}$$

where

$V_{x,y}$ is the grey level at point (x, y);

x is the index along x-axis.

6.2.3.3 Determining the proportion of misclassified pixels

Formula (17) specifies the calculation of the proportion of pixels misclassified respectively as valley, and Formula (18) specifies the calculation of the proportion of pixels misclassified as ridge.

$$\alpha = \frac{v_B}{v_T} \tag{17}$$

$$\beta = \frac{r_B}{r_T} \tag{18}$$

where

α is the proportion of pixels misclassified as valley;

β is the proportion of pixels misclassified as ridge;

v_B is the number of pixels in the valley region with intensity lower than DT;

v_T is the total number of pixels in the valley region;

r_B is the number of pixels in the ridge region with intensity higher than DT;

r_T is the total number of pixels in the ridge region.

6.2.3.4 Determining the normalized ridge and valley width

The normalized valley width $\overline{W}_v$ and the normalized ridge width $\overline{W}_r$ are determined according to Formulae (19) and (20):

$$\overline{W}_v = \frac{W_v}{\left(\frac{S \times 2,54}{125}\right)W^{\max}} \tag{19}$$

$$\overline{W}_r = \frac{W_r}{\left(\frac{S \times 2,54}{125}\right)W^{\max}} \tag{20}$$

where

S	is the spatial sampling rate in pixels per centimetre of the capture device;
$W^{\max}$	is the estimated ridge or valley width for an image with 49,21 pixels per centimetre (125 pixels per inch) spatial sampling rate;
W_v and W_r	are the observed valley and ridge widths, respectively.

According to Reference [2], $W^{\max} = 5$ is reasonable for 49,21 pixels per centimetre (125 pixels per inch) spatial sampling rate. By extension, $\left(\frac{S \times 2,54}{125}\right)W^{\max}$ is 20 for a spatial sampling rate of 196,85 pixels per centimetre (500 pixels per inch).

6.2.3.5 Computing the local clarity

The local quality value $q_{\mathrm{LCL}}^{\mathrm{local}}$ is the constrained average value of α and β with a range between 0 and 1, as shown in Formula (21):

$$q_{\mathrm{LCL}}^{\mathrm{local}} = \begin{cases} 1 - \frac{\alpha + \beta}{2}, & \text{if } \left(W_v^{\mathrm{nmin}} < \overline{W}_v < W_v^{\mathrm{nmax}}\right), \left(W_r^{\mathrm{nmin}} < \overline{W}_r < W_r^{\mathrm{nmax}}\right) \\ 0, & \text{otherwise.} \end{cases} \tag{21}$$

where W_r^{nmin} and W_v^{nmin} are the minimum values for the normalized ridge and valley width, calculated according to Formulae (22) and (23) respectively:

$$W_r^{\mathrm{nmin}} = \frac{3}{\overline{W}_r} \tag{22}$$

$$W_v^{\mathrm{nmin}} = \frac{2}{\overline{W}_v} \tag{23}$$

and where W_r^{nmax} and W_v^{nmax} are the maximum values for the normalized ridge and valley width, calculated according to Formulae (24) and (25) respectively:

$$W_r^{\mathrm{nmax}} = \frac{10}{\overline{W}_r} \tag{24}$$

$$W_v^{\mathrm{nmax}} = \frac{10}{\overline{W}_v} \tag{25}$$

NOTE   Particular regions inherent in a fingerprint will negatively affect q_{LCL}^{local}. For example, ridge endings and bifurcations or areas with high curvature such as those commonly found in core and delta points.

6.2.3.6   LCL algorithm

For each local region V in I:

a)   rotate V such that dominant ridge flow is perpendicular to x-axis using nearest neighbour interpolation;

b)   crop rotated V such that no invalid regions are included;

c)   with V obtain the ridge-valley signature S (6.2.3.2);

d)   determine DT using linear regression on S;

e)   for each element $S(x)$, set threshold $T(x)$ of x being ridge or valley based on DT;

f)   classify columns in V as ridge (1) or valley (0) with $P(x) = \begin{cases} 1, & \text{if } S(x) < T(x) \\ 0, & \text{otherwise.} \end{cases}$;

g)   determine ridge-valley transition vector C from P;

h)   compute the vector W containing ridge and valley widths from C;

i)   determine normalized ridge width and valley width $\overline{W}_r$ and $\overline{W}_v$ (6.2.3.4);

j)   determine the proportion of misclassified pixels α and β (6.2.3.3);

k)   compute the local quality value q_{LCL}^{local} (6.2.3.5).

NOTE   The reference implementation fills invalid regions with 0-valued pixels.

Figure 4 visualizes the processing steps.

a) Crop of current local region

b) Average profile of local region

c) Average local region profile with linear regression line

d) Binarisation mask with ridge and valley regions based on regression line

e) Pixels determined to be ridge based on mask

f) Pixels misclassified as valley based on the threshold

g) Pixels determined to be valley based on mask

h) Pixels misclassified as ridge based on the threshold

i) Local clarities

Key

X   block x-index

Y   mean intensity
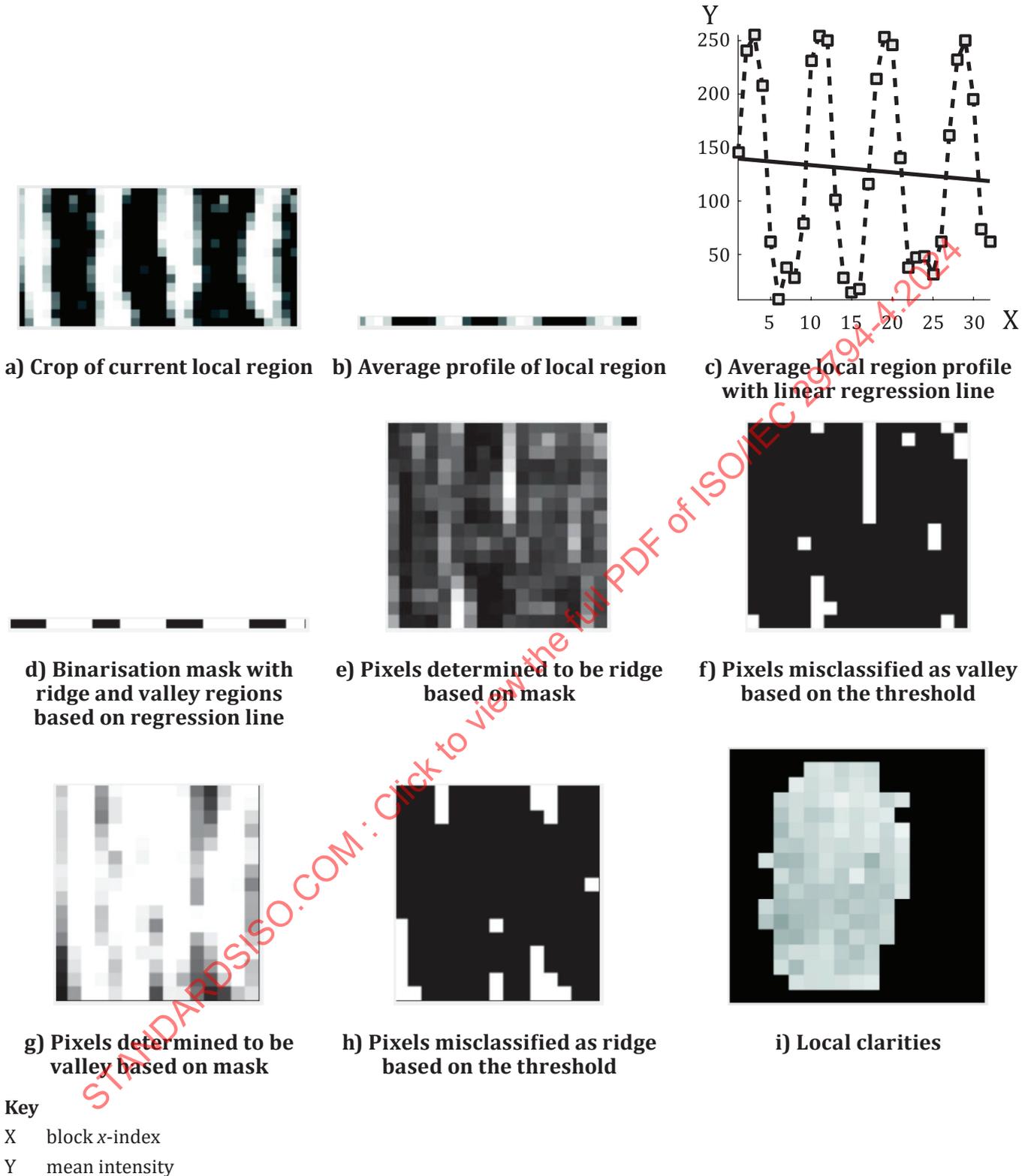
Figure 4 — Processing steps of local clarity algorithm

6.2.4 Frequency domain analysis (FDA)

6.2.4.1 Description

Frequency domain analysis (FDA) computes local quality and operates in a block-wise manner. A one-dimensional signature of the ridge-valley structure is extracted and the discrete Fourier transform (DFT) is computed on the signature to determine the frequency of the sinusoid following the ridge-valley structure.[6]

The ridge-valley signature of a high quality sample is a periodic signal, which can be approximated either by a square wave or a sinusoidal wave. In the frequency domain, an ideal square wave should exhibit a dominant frequency with sideband frequency components (sinc function). A sinusoidal wave consists of one dominant frequency and minimum components at other non-dominant frequencies.

For each local region, a signature perpendicular to the dominant ridge flow orientation is computed.

The FDA described in 6.2.4 computes the one-dimensional signatures by performing averaging along the ridge flow direction. The averaging process filters out noise along the ridge and valley flow and provides a modelling of a smooth changing signal in a direction perpendicular to ridge flow.

6.2.4.2 Computing the local FDA quality component

The local quality value is computed by using Formula (26):

$$q_{\mathrm{FDA}}^{\mathrm{local}} = \begin{cases} 1, & \text{if } F_{\max} = A_1 \text{ or } F_{\max} = A_{|A|} \\ \dfrac{A_{F_{\max}} + C\left(A_{F_{\max}-1} + A_{F_{\max}+1}\right)}{\sum_{F=1}^{|A|/2} A_F}, & \text{otherwise.} \end{cases} \tag{26}$$

where

　　$0{,}3$　is the attenuation parameter C;

　　A_x　is the amplitude at frequency index x.

The value of $q_{\mathrm{FDA}}^{\mathrm{local}}$ is set to 1 when the maximum frequency, $F_{\max}$, amplitude occurs at index $F_{\max} = A_1$ or $F_{\max} = A_{|A|}$.

6.2.4.3 FDA algorithm

For each local region V in I:

a)　pad V with a 2-pixel border;

b)　rotate V with nearest neighbour interpolation such that dominant ridge flow is perpendicular to the x-axis with nearest neighbour interpolation;

c)　crop V such that no invalid regions are included;

d)　with V, obtain the ridge-valley signature S (6.2.3.2);

e)　compute the DFT of S to obtain the magnitude representation A;

f)　discard the DC component (i.e. the first component of A);

g)　determine $F_{\max}$ as the index with the largest magnitude in A;

h)　compute $q_{\mathrm{FDA}}^{\mathrm{local}}$ of V using A and $F_{\max}$ (6.2.4.2).

NOTE　　　The reference implementation fills invalid regions with 0-valued pixels.

Figure 5 visualizes the processing steps.

a) Central area of input local region

b) Ridge-valley profile

c) DFT of ridge-valley profile

d) Map of $q_{\text{FDA}}^{\text{local}}$
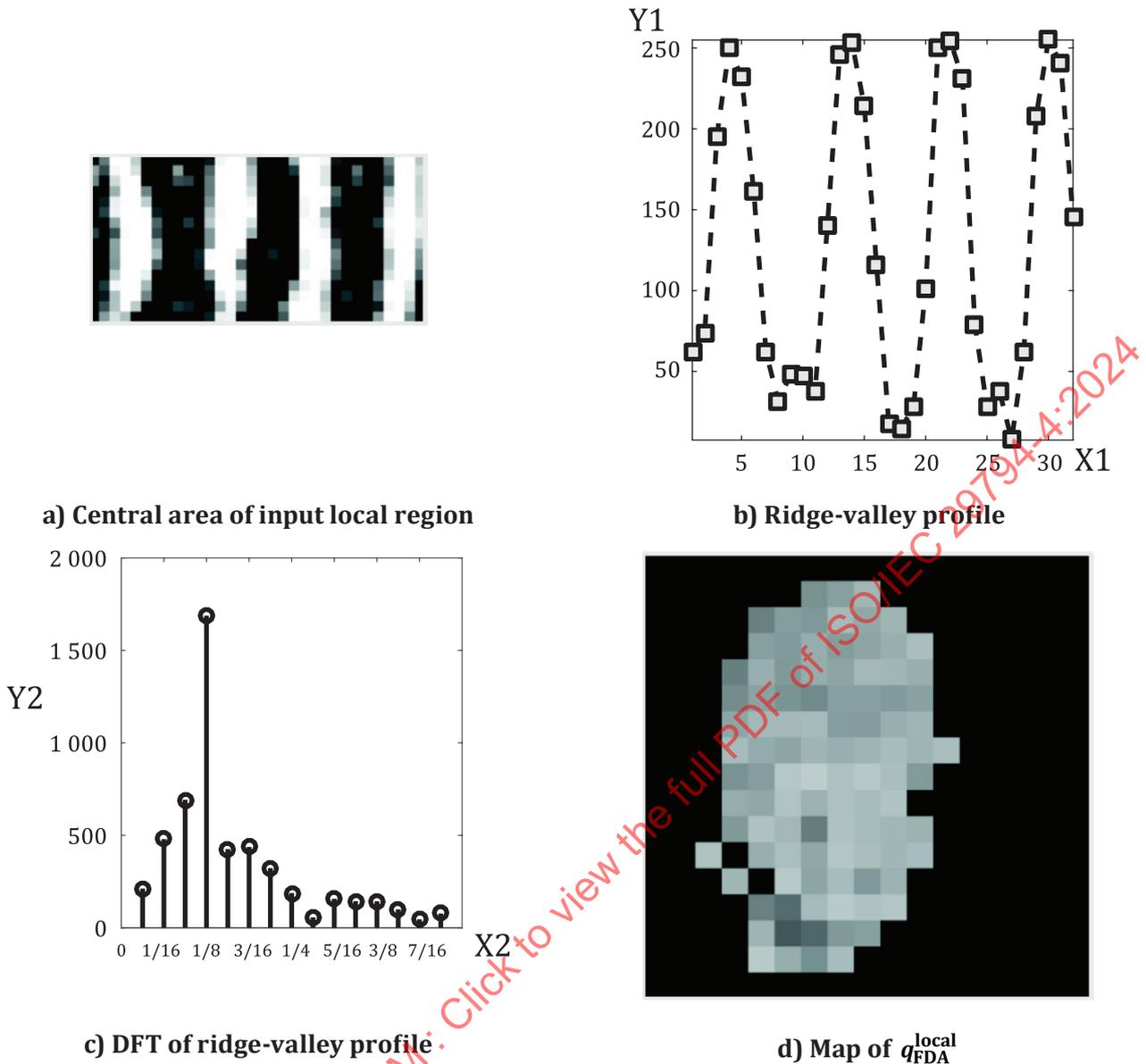
Key

X1   mean intensity

Y1   block *x*-index

X2   magnitude

Y2   cycle/pixel

Figure 5 — Processing steps of FDA quality algorithm

6.2.5 Ridge valley uniformity

6.2.5.1 Feature description

Ridge valley uniformity (RVU) is a measure of the consistency of the ridge and valley widths.[3]. The expectation for finger image with clear ridge and valley separation is that the ratio between ridge and valley widths remains fairly constant throughout the finger image.

The ratio of ridge thickness to valley thickness should be constant and close to 1 throughout the whole image for a good quality finger image. The feature computes local quality and operates in a block-wise manner.

NOTE   The ridge valley uniformity depends on the spatial sampling rate.

6.2.5.2   RVU algorithm

For each local region V in I:

a)   determine dominant ridge flow orientation $\mathrm{angle}(V)$ of V;

b)   rotate V such that $\mathrm{angle}(V)$ is perpendicular to x-axis;

c)   crop V such that no invalid regions are included;

d)   with V, obtain the ridge-valley signature S (6.2.3.2);

e)   determine DT using linear regression on S;

f)   for each $S(x)$, compute threshold $T(x) = x \times \mathrm{DT}(1) + \mathrm{DT}(0)$;

g)   binarize S using T;

h)   classify ridge and valley in S as $P(x) = \begin{cases} 1, \text{if } S(x-1) < T(x) \\ 0, \text{otherwise.} \end{cases}$;

i)   compute ridge-valley transition vector as $C(x) = \begin{cases} 1, \text{if } P(x-1) \neq P(x) \\ 0, \text{otherwise.} \end{cases}$;

j)   drop first and last transition from S using C to remove incomplete ridges or valleys and obtain S';

k)   compute $q_{\mathrm{RVU}}^{\mathrm{local}}$ as the ratio of the width of ridges against valleys in S'.

Figure 6 visualizes the processing steps.
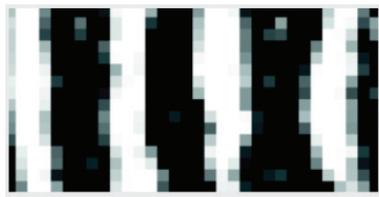
a) Crop of current local region

b) Average profile of local region
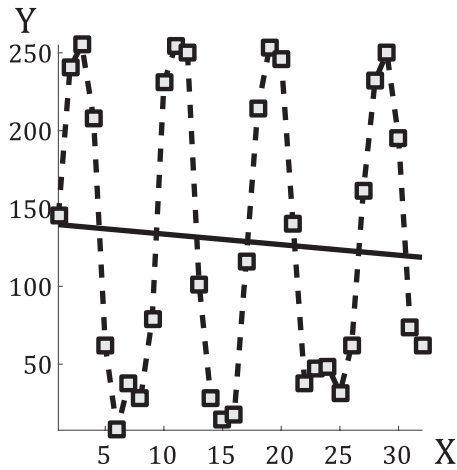
c) Average profile with regression line

d) Local native quality component values displayed as the ratio of the width of ridges against valleys

Key

X   block *x*-index

Y   mean intensity

Figure 6 — Processing steps of ridge valley uniformity quality algorithm

6.2.6   Orientation flow

6.2.6.1   Description

Orientation flow (OFL)[4] is a measure of ridge flow continuity which is based on the absolute orientation difference between a local region and its 8-neighbourhood of local regions.

Orientation flow is a good indicator to describe the quality of a good fingerprint pattern because, in general, the flow of the ridge direction changes gradually, except in an area with a delta or a core. The feature computes local quality and operates in a block-wise manner.

6.2.6.2 Local region-wise absolute orientation difference

The ridge flow is determined as a measure of the absolute difference between a local region and its neighbouring local regions. The absolute difference $D(i,j)$ for local region $V(i,j)$ is computed using the dominant ridge flow orientations of this local region and of its neighbours, as shown in Formula (27):

$$D(i,j) = \frac{\sum_{m=-1}^{1}\sum_{n=-1}^{1}\min\left(\left|\theta_{V(i,j)}-\theta_{V(i-m,j-n)}\right|, 360° - \left|\theta_{V(i,j)}-\theta_{V(i-m,j-n)}\right|\right)}{8} \tag{27}$$

Formula (27)[2] takes the minimum angle differences and 360° minus the angle difference because of the circularity of angles (e.g. the difference between angles of 2° and 358° is 4°).

6.2.6.3 Local orientation flow quality

The local orientation quality $q_{\text{OFL}}^{\text{local}}$ for the local region orientation difference $D(i,j)$ is calculated according to Formula (28):

$$q_{\text{OFL}}^{\text{local}} = \begin{cases} \dfrac{D(i,j)-\theta_{\min}}{90°-\theta_{\min}}, & \text{if } D(i,j) > \theta_{\min} \\ 0, & \text{otherwise.} \end{cases} \tag{28}$$

where $\theta_{\min} = 4°$ is the threshold for minimum angle difference to consider and the units of $D(i,j)$ are degrees.

6.2.6.4 OFL algorithm

a)   Determine the dominant ridge flow orientation $\text{angle}(V)$ of local region V and I.

b)   For each local region V in I:

   1)   compute the absolute orientation difference $D(i,j)$ using $\text{angle}(V)$ (6.2.6.2);

   2)   compute the local orientation quality $q_{\text{OFL}}^{\text{local}}$ (6.2.6.3).

Figure 7 visualizes the processing steps.

a) Normal (perpendicu-lar) line to the ridgeline orientation   **b) Local orientations**   **c) Orientation differences**   **d) Local quality values**
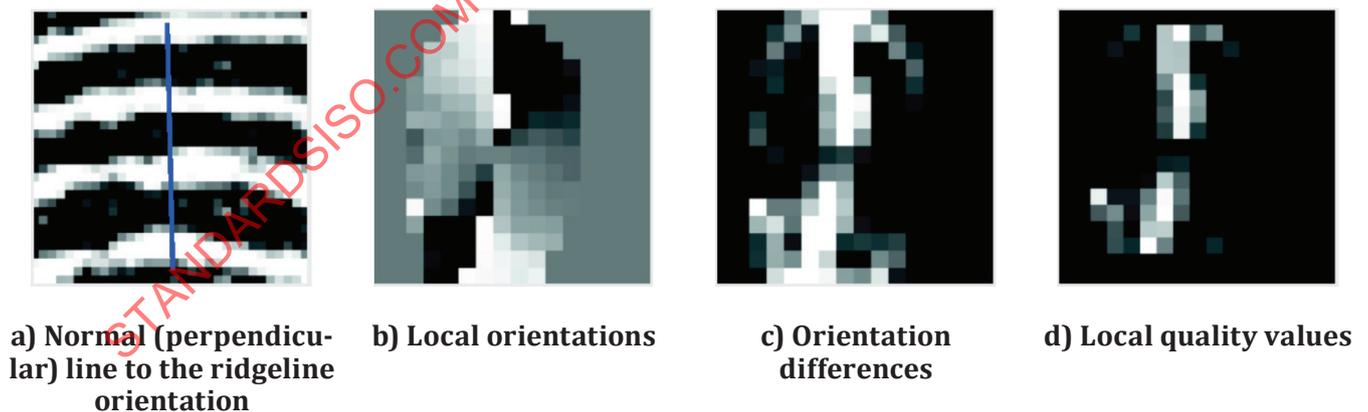
Figure 7 — Processing steps of orientation flow quality algorithm

6.2.7 MU

6.2.7.1 Description

MU is the arithmetic mean of the pixel intensities of all pixels in the input image. The feature computes global quality.

6.2.7.2 MU algorithm

Compute Q_{MU} as the arithmetic mean of pixel intensities in $\boldsymbol{I}$.

6.2.7.3 Mapping to the desired value range

To fit into a quality block as specified in ISO/IEC 29794-1, the floating-point q_{MU} values shall be mapped to a quality component Q_{MU} in the range from 0 to 100 using Formula (2), where x is q_{MU}, $\min(q_{MU})$ is 0 and $\max(q_{MU})$ is 255. See Formula (29).

$$Q_{MU} = \left\lfloor \frac{q_{MU}}{255 + \varepsilon} 101 \right\rfloor \tag{29}$$

6.2.8 MMB

6.2.8.1 Description

MMB is the arithmetic mean of all local region arithmetic means in the greyscale input image. The feature computes local quality and operates in a block-wise manner.

6.2.8.2 MMB algorithm

a) For each local region $\boldsymbol{V}$ in $\boldsymbol{I}$:

    1) compute the arithmetic mean of the pixel intensities in $\boldsymbol{V}$ as q_{MMB}^{local}.

b) Compute Q_{MMB} as the arithmetic mean of set of q_{MMB}^{local}.

6.2.8.3 Mapping to the desired value range

To fit into a quality block as specified in ISO/IEC 29794-1, the floating-point q_{MMB} values shall be mapped to a quality component Q_{MMB} in the range from 0 to 100 using Formula (2), where x is q_{MMB}, $\min(q_{MMB})$ is 0 and $\max(q_{MMB})$ is 255. See Formula (30).

$$Q_{MMB} = \left\lfloor \frac{q_{MMB}}{255 + \varepsilon} 101 \right\rfloor \tag{30}$$

6.2.9 Minutiae count in finger image

6.2.9.1 Description

FingerJet Fingerprint Feature Extractor, Open Source Edition (FJFX)[5] is the minutiae extractor selected for the reference implementation due to licensing conditions (including commercial use cases and redistribution), computational complexity, and platform independence. FJFX provides a count of detected minutiae in the finger image. The minutiae count has a bearing on the mated comparison score. The feature computes global quality.

6.2.9.2 MIN$^{\text{CNT}}$ algorithm

$q_{\text{MIN}}^{\text{CNT}}$ is the number of detected minutiae in the finger image as determined by the minutiae extractor.

6.2.9.3 Mapping to the desired value range

To fit into a quality block as specified in ISO/IEC 29794-1, the $q_{\text{MIN}}^{\text{CNT}}$ values shall be limited to 100 using Formula (31), yielding the quality component $Q_{\text{MIN}}^{\text{CNT}}$:

$$Q_{\text{MIN}}^{\text{CNT}} = \begin{cases} q_{\text{MIN}}^{\text{CNT}} & \text{if } q_{\text{MIN}}^{\text{CNT}} \leq 100 \\ 100 & \text{if } q_{\text{MIN}}^{\text{CNT}} > 100 \end{cases} \tag{31}$$

6.2.10 Minutiae count in centre of mass region

6.2.10.1 Description

This quality component is the minutiae count in a (200 × 200) pixels local region centred on the centre of mass of the detected minutiae as described in 6.2.9. The quality component computes local quality at the minutiae locations.

6.2.10.2 MIN$^{\text{COM}}$ algorithm

$q_{\text{MIN}}^{\text{COM}}$ is the number of minutiae occurring within a (200 × 200) pixels local region centred at the centre of mass of the locations of all detected minutiae in the finger image as described in 6.2.9.

6.2.10.3 Mapping to the desired value range

To fit into a quality block as specified in ISO/IEC 29794-1, the floating-point $q_{\text{MIN}}^{\text{COM}}$ values shall be limited to 100 using Formula (32), yielding the quality component $Q_{\text{MIN}}^{\text{COM}}$:

$$Q_{\text{MIN}}^{\text{COM}} = \begin{cases} q_{\text{MIN}}^{\text{COM}} & \text{if } q_{\text{MIN}}^{\text{COM}} \leq 100 \\ 100 & \text{if } q_{\text{MIN}}^{\text{COM}} > 100 \end{cases} \tag{32}$$

6.2.11 Minutiae quality based on local image mean

6.2.11.1 Description

For each minutia location detected as described in 6.2.9, a local quality based on image statistics is computed. The reported quality value is aggregated as the count of local qualities which occurs in the specified range. The feature computes local quality at the minutiae locations.

6.2.11.2 MIN$^{\text{MU}}$ algorithm

$q_{\text{MIN}}^{\text{MU}}$ is computed by first determining the local quality of each minutia detected as described in 6.2.9, using Formula (33):

$$q_{\text{MIN}}^{\text{local}_{\text{MU}}} = \frac{\mu(I) - \mu(V)}{\sigma(I)} \tag{33}$$

where

$\mu(I)$ is the arithmetic mean of the finger image;

$\mu(V)$ is the arithmetic mean of a (32 × 32) pixels local region centred on the minutia;

$\sigma(I)$ is the standard deviation of the finger image.

$q_{\text{MIN}}^{\text{MU}}$ is finally computed as the percentage of $q_{\text{MIN}}^{\text{local}_{\text{MU}}}$ values greater than 0 and less than or equal to 0,5, as shown in Formula (34):

$$q_{\text{MIN}}^{\text{MU}} = \frac{\sum_{x=1}^{q_{\text{MIN}}^{\text{CNT}}} \begin{cases} 1, 0 < q_{\text{MIN}_x}^{\text{local}_{\text{MU}}} \leq 0,5 \\ 0, \text{otherwise.} \end{cases}}{q_{\text{MIN}}^{\text{CNT}}} \tag{34}$$

6.2.11.3 Mapping to the desired value range

To fit into a quality block as specified in ISO/IEC 29794-1, the floating-point $q_{\text{MIN}}^{\text{MU}}$ values shall be mapped to a quality component $Q_{\text{MIN}}^{\text{MU}}$ in the range from 0 to 100 by multiplication with 100, using Formula (2), where x is $q_{\text{MIN}}^{\text{MU}}$, $\min\left(q_{\text{MIN}}^{\text{MU}}\right)$ is 0 and $\max\left(q_{\text{MIN}}^{\text{MU}}\right)$ is 255. See Formula (35).

$$Q_{\text{MIN}}^{\text{MU}} = \left\lfloor \frac{q_{\text{MIN}}^{\text{MU}}}{255 + \varepsilon} 101 \right\rfloor \tag{35}$$

6.2.12 Minutiae quality based on local orientation certainty level

6.2.12.1 Description

For each minutia location detected, as described in 6.2.9, a local orientation certainty level is computed. The reported quality value is aggregated as the count of local qualities which exceed the specified value. The feature computes local quality at the minutiae locations.

6.2.12.2 MIN$^{\text{OCL}}$ algorithm

$q_{\text{MIN}}^{\text{OCL}}$ is computed by first determining the local quality of each minutia detected as described in 6.2.9 as shown in Formula (36):

$$q_{\text{MIN}}^{\text{local}_{\text{OCL}}} = q_{\text{OCL}}^{\text{local}}(V) \tag{36}$$

where $q_{\text{OCL}}^{\text{local}}(V)$ is the local orientation certainty level (6.2.2) for the (32 × 32) pixels local region V centred on the minutia.

$q_{\text{MIN}}^{\text{OCL}}$ is finally computed as the percentage of $q_{\text{MIN}}^{\text{local}_{\text{OCL}}}$ values greater than 0,8, as shown in Formula (37):

$$q_{\text{MIN}}^{\text{OCL}} = \frac{\sum_{x=1}^{q_{\text{MIN}}^{\text{CNT}}} \begin{cases} 1, q_{\text{MIN}_x}^{\text{local}_{\text{OCL}}} > 0,8 \\ 0, \text{otherwise.} \end{cases}}{q_{\text{MIN}}^{\text{CNT}}} \qquad (37)$$

6.2.12.3 Mapping to the desired value range

To fit into a quality block as specified in ISO/IEC 29794-1, the floating-point $q_{\text{MIN}}^{\text{OCL}}$ values shall be mapped to a quality component $Q_{\text{MIN}}^{\text{OCL}}$ in the range from 0 to 100 by multiplication with 100, using Formula (2), where x is $q_{\text{MIN}}^{\text{OCL}}$, $\min\left(q_{\text{MIN}}^{\text{OCL}}\right)$ is 0 and $\max\left(q_{\text{MIN}}^{\text{OCL}}\right)$ is 1, as shown in Formula (38):

$$Q_{\text{MIN}}^{\text{OCL}} = \left\lfloor \frac{q_{\text{MIN}}^{\text{OCL}}}{1+\varepsilon} 101 \right\rfloor \qquad (38)$$

6.2.13 Region of interest image mean

6.2.13.1 Description

The region of interest for the finger image is the foreground region of the image containing the fingerprint. The mean pixel intensity in this area is computed over the set of (32 × 32) pixels local regions which have a least one pixel contained in the region of interest. The feature computes global quality.

NOTE   The quality component is highly correlated with q_{MU} (6.2.7) and q_{MMB} (6.2.8).

6.2.13.2 Determine the region of interest

a) Erode the finger image I with a 5 × 5 structuring element to obtain $\bar{I}$.

b) Apply normalized Gaussian blur filter (each weight is divided by the sum of all weights) with kernel size 41 × 41 and standard deviation of 6,5 to $\bar{I}$ to obtain G.

c) Binarize G to obtain B.

   NOTE   The reference implementation uses Otsu's method[7] for binarization.

d) Apply normalized Gaussian blur filter (each weight is divided by the sum of all weights) with kernel size 91 × 91 and standard deviation of 14,0 to B to obtain G'.

e) Binarize G' using Otsu's method to obtain B'.

f) Determine the contours of inverted B' to obtain C.

   NOTE   The reference implementation uses Suzuki's method[8] for determining contours.

g) Contours in the hierarchy of C that have a parent shall be set to 0 valued pixels.

h) 0 valued pixel regions that are not the largest 0 valued pixel area shall be set to 1 valued pixels.

i) The resulting binary mask R contains the region of interest as a region of 0 valued pixels.

Figure 8 visualizes the processing steps.

a) Original image I b) Eroded image $\bar{I}$ c) Blurred image G d) Binarized image B

e) Blurred image G' f) Binarized image B' g) Contours of C outlined in different colours   h) Region of interest mask R
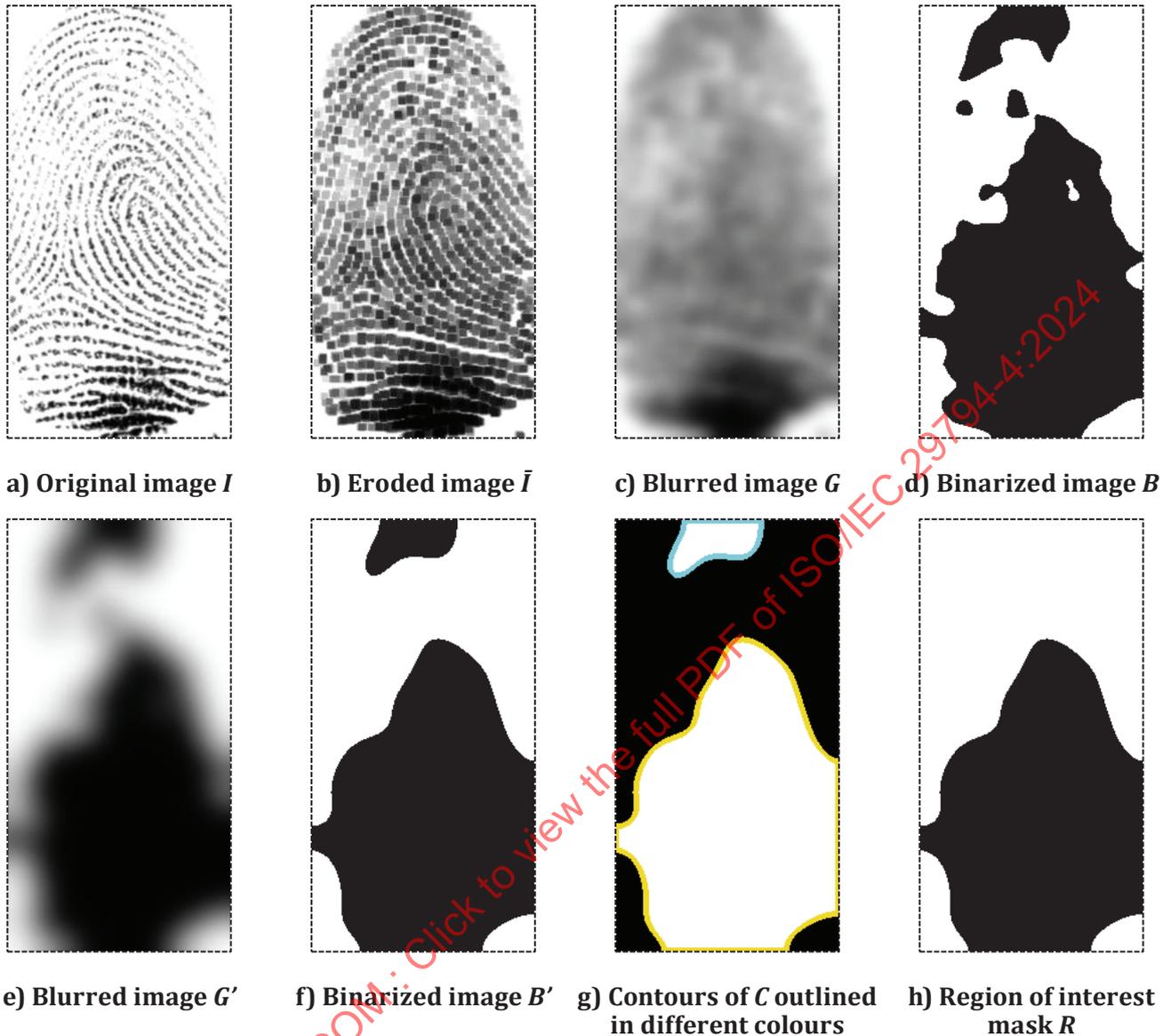
NOTE   Each subfigure contains a dashed black border.

Figure 8 — Processing steps of region of interest algorithm

6.2.13.3 AREA algorithm

a) Determine the region of interest R ([6.2.13.2](#)).

b) For each 32 × 32 local region V in I:

   1)   if V has at least 1 pixel contained in foreground of R, mark the local region as foreground.

   NOTE   Up to and including in version NFIQ 2.2, V is implemented as a (16 × 16) pixels region. The values, however, are the same as when local regions of size (32 × 32) pixels are used.

c) Compute q_{AREA}^{μ} as the arithmetic mean of the grey levels of all pixels in the set of local regions V marked as foreground.

6.2.13.4 Mapping to the desired value range

To fit into a quality block as specified in ISO/IEC 29794-1, the floating-point q_{AREA}^{μ} values shall be mapped to a quality component Q_{AREA}^{μ} in the range from 0 to 100 using Formula (2), where x is q_{AREA}^{μ}, $\min\left(q_{\text{AREA}}^{\mu}\right)$ is 0 and $\max\left(q_{\text{AREA}}^{\mu}\right)$ is 255, as shown in Formula (39):

$$Q_{\text{AREA}}^{\mu} = \left\lfloor \frac{q_{\text{AREA}}^{\mu}}{255+\varepsilon} 101 \right\rfloor \tag{39}$$

6.2.14 Region of interest orientation map coherence sum

6.2.14.1 Description

The orientation map coherence sum quantifies the coherence of the estimated finger image orientation field. The coherence map is computed according to the coherence method specified in Reference [9]. The feature computes local quality and operates in a block-wise manner.

6.2.14.2 Computing the gradient field

The gradient field $\boldsymbol{g} = \left(g_x, g_y\right)^T$ of pixel intensity $\boldsymbol{I}(i,j)$ of $\boldsymbol{I}$ is as shown in Formulae (40) and (41):

$$
\begin{aligned}
g_x(i,j) &= \boldsymbol{I}(i+1,j) - \boldsymbol{I}(i-1,j))/2 & \text{for} \quad 1 \le i \le \boldsymbol{I}_{\text{w}} -1, 0 \le j \le \boldsymbol{I}_{\text{h}} \\
g_x(0,j) &= \boldsymbol{I}(1,j) - \boldsymbol{I}(0,j) & \text{for} \quad 0 \le j \le \boldsymbol{I}_{\text{h}} \\
g_x(\boldsymbol{I}_{\text{w}},j) &= I(\boldsymbol{I}_{\text{w}},j) - I(\boldsymbol{I}_{\text{w}}-1,j) & \text{for} \quad 0 \le j \le \boldsymbol{I}_{\text{h}}
\end{aligned}
\tag{40}
$$

and

$$
\begin{aligned}
g_y(i,j) &= (\boldsymbol{I}(i,j+1) - \boldsymbol{I}(i,j-1))/2 & \text{for} \quad 0 \le i \le \boldsymbol{I}_{\text{w}}, 1 \le j \le \boldsymbol{I}_{\text{h}} -1 \\
g_y(i,0) &= \boldsymbol{I}(i,1) - \boldsymbol{I}(i,0) & \text{for} \quad 0 \le i \le \boldsymbol{I}_{\text{w}} \\
g_y(i,\boldsymbol{I}_{\text{h}}) &= \boldsymbol{I}(i,\boldsymbol{I}_{\text{h}}) - \boldsymbol{I}(i,\boldsymbol{I}_{\text{h}}-1) & \text{for} \quad 0 \le i \le \boldsymbol{I}_{\text{w}}
\end{aligned}
\tag{41}
$$

where $\boldsymbol{I}_{\text{w}}$ and $\boldsymbol{I}_{\text{h}}$ are respectively the width and height of $\boldsymbol{I}$ in pixels.

6.2.14.3 Computing the coherence of a local region

The coherence of a local region $\boldsymbol{V}$ is computed from its pixel-intensity gradient field $\boldsymbol{g}_{\text{s}}$ as shown in Formula (42):

$$\text{coh}(\boldsymbol{V}) = \frac{\left|\sum \boldsymbol{g}_{\text{s}}(i,j)\right|}{\sum \left|\boldsymbol{g}_{\text{s}}(i,j)\right|} \tag{42}$$

where $|x|$ denotes the Euclidean norm of x and the sums are taken over all pixels in $\boldsymbol{V}$.

NOTE $\boldsymbol{g}_{\text{s}}$ is defined in 6.2.14.4.

6.2.14.4 COH$^{\text{SUM}}$ algorithm

a)   Compute the pixel-intensity gradient field $\boldsymbol{g}$ of $\boldsymbol{I}$ (6.2.14.2).

b)   Compute the square gradient field as $\boldsymbol{g}_s = \left(g_x^2 - g_y^2, 2g_x g_y\right)^T$.

c)   Determine the region of interest $\boldsymbol{R}$ (6.2.13.2).

d) For each (16 × 16) pixels local region $\boldsymbol{V}$ in $\boldsymbol{I}$:

    1) if $\boldsymbol{V}$ has at least 1 pixel contained in foreground of $\boldsymbol{R}$, compute the coherence of $\boldsymbol{V}$ as $\mathrm{coh}(\boldsymbol{V})$, otherwise set $\mathrm{coh}(\boldsymbol{V}) = 0$.

    NOTE   Up to and including in version NFIQ 2.2, $\boldsymbol{V}$ is implemented as a (16 × 16) pixels region.

e) Compute $q_{\mathrm{COH}}^{\mathrm{sum}}$ as the sum of the $\mathrm{coh}(\boldsymbol{V})$ of all $\boldsymbol{V}$.

6.2.14.5 Mapping to the desired value range

To fit into a quality block as specified in ISO/IEC 29794-1, the floating point $q_{\mathrm{COH}}^{\mathrm{sum}}$ values shall be mapped to a quality component $Q_{\mathrm{COH}}^{\mathrm{sum}}$ in the range from 0 to 100 and rounded to the nearest integer using Formula (2), where x is $q_{\mathrm{COH}}^{\mathrm{sum}}$, $\min\left(q_{\mathrm{COH}}^{\mathrm{sum}}\right)$ is 0 and $\max\left(q_{\mathrm{COH}}^{\mathrm{sum}}\right)$ is 3 150. See Formula (43):

$$Q_{\mathrm{COH}}^{\mathrm{sum}} = \left\lfloor \frac{q_{\mathrm{COH}}^{\mathrm{sum}}}{3\,150 + \varepsilon}\,101 \right\rfloor \tag{43}$$

NOTE $q_{\mathrm{COH}}^{\mathrm{REL}}$ (6.2.15.2) is a value between 0,0 and 1,0. The reference implementation's minutiae extractor implementation defined in 6.2.9 imposes a maximum image size of (800 × 1 000) pixels, which can fit 3 150 (16 × 16) pixels blocks. Therefore, the maximum value of $q_{\mathrm{COH}}^{\mathrm{sum}}$ in the reference implementation is 3 150. The value of $q_{\mathrm{COH}}^{\mathrm{sum}}$ between 0 and 3 150 can therefore be normalized to derive $Q_{\mathrm{COH}}^{\mathrm{sum}}$.

6.2.15 Region of interest relative orientation map coherence sum

6.2.15.1 Description

The relative orientation map coherence sum is the average of local region orientation coherence as determined by 6.2.14. The feature computes local quality and operates in a block-wise manner.

6.2.15.2 COH^REL algorithm

a) Compute $q_{\mathrm{COH}}^{\mathrm{sum}}$ and store the number of local regions $\boldsymbol{V}$ which have at least one pixel contained in $\boldsymbol{R}$ as n (6.2.14).

b) Compute $q_{\mathrm{COH}}^{\mathrm{REL}} = \dfrac{q_{\mathrm{COH}}^{\mathrm{sum}}}{n}$.

6.2.15.3 Mapping to the desired value range

To fit into a quality block as specified in ISO/IEC 29794-1, the floating-point $q_{\mathrm{COH}}^{\mathrm{REL}}$ values shall be mapped to a quality component $Q_{\mathrm{COH}}^{\mathrm{REL}}$ in the range from 0 to 100 using Formula (2), x is $q_{\mathrm{COH}}^{\mathrm{REL}}$, $\min\left(q_{\mathrm{COH}}^{\mathrm{REL}}\right)$ is 0 and $\max\left(q_{\mathrm{COH}}^{\mathrm{REL}}\right)$ is 1, as shown in Formula (44):

$$Q_{\mathrm{COH}}^{\mathrm{REL}} = \left\lfloor \frac{q_{\mathrm{COH}}^{\mathrm{REL}}}{1 + \varepsilon}\,101 \right\rfloor \tag{44}$$

6.2.16 Quality feature vector composition

6.2.16.1 Description

Quality features specified in 6.2.2 to 6.2.6 provide a map of values for local regions in the finger image. The quality features specified in 6.2.7 to 6.2.15 provide scalar quality values for the finger image.

The specified features shall be composed such that a fixed length feature vector is obtained for use by a classification system. Thus, the features in 6.2.2 to 6.2.6 are aggregated using arithmetic mean specified in 6.2.16.2, standard deviation specified in 6.2.16.3 and histogram specified in 6.2.16.4 for inclusion in the final feature vector specified in 6.2.16.5.

6.2.16.2 Mean of local quality values

6.2.16.2.1 Basic calculation

The mean quality value over an $N \times M$ matrix of local quality values is computed as shown in Formula (45):

$$G = \frac{1}{N \times M} \sum_{i=1}^{N} \sum_{j=1}^{M} L(i,j) \tag{45}$$

where

L are local quality values q_{OCL}^{local} (6.2.2), q_{LCL}^{local} (6.2.3), q_{FDA}^{local} (6.2.4), q_{RVU}^{local} (6.2.5), or q_{OFL}^{local} (6.2.6);

G are the aggregated mean quality values q_{OCL}^{μ}, q_{LCL}^{μ}, q_{FDA}^{μ}, q_{RVU}^{μ}, or q_{OFL}^{μ}, in respect of L.

6.2.16.2.2 Mapping to the desired value range

To fit into a quality block as specified in ISO/IEC 29794-1, the floating-point aggregated mean quality values produced in 6.2.16.2.1 shall be mapped to a quality component in the range from 0 to 100 and rounded to the nearest integer.

For q_{OCL}^{μ}, q_{LCL}^{μ}, q_{FDA}^{μ} and q_{OFL}^{μ}, refer to Formula (2) from 6.1.2.1 to yield Q_{OCL}^{μ}, Q_{LCL}^{μ}, Q_{FDA}^{μ} and Q_{OFL}^{μ}, respectively. For q_{RVU}^{μ}, Formula (46) shall be used for mapping to yield Q_{RVU}^{μ}:

$$Q_{RVU}^{\mu} = \left\lfloor 100 \cdot \text{sigmoid}\left(q_{RVU}^{\mu}, 1, \frac{1}{2}\right) + \frac{1}{2} \right\rfloor \tag{46}$$

6.2.16.3 Standard deviation of local quality values

6.2.16.3.1 Basic calculation

The standard deviation over an $N \times M$ matrix of local quality values is computed as shown in Formula (47):

$$G = \left(\frac{1}{N \times M - 1} \sum_{i=1}^{N} \sum_{j=1}^{M} \left(L(i,j) - F \right)^2 \right)^{\frac{1}{2}} \tag{47}$$

where

L are local quality values q_{OCL}^{local} (6.2.2), q_{LCL}^{local} (6.2.3), q_{FDA}^{local} (6.2.4), q_{RVU}^{local} (6.2.5), or q_{OFL}^{local} (6.2.6);

G are the aggregated standard deviation quality values q_{OCL}^{σ}, q_{LCL}^{σ}, q_{FDA}^{σ}, q_{RVU}^{σ}, or q_{OFL}^{σ}, in respect of L;

F are the aggregated mean quality values q_{OCL}^{μ}, q_{LCL}^{μ}, q_{FDA}^{μ}, q_{RVU}^{μ}, or q_{OFL}^{μ}, in respect of L.

6.2.16.3.2 Mapping to the desired value range

To fit into a quality block as specified in ISO/IEC 29794-1, the floating-point aggregated standard deviation quality values produced in 6.2.16.3.1 shall be mapped to a quality component in the range from 0 to 100 and rounded to the nearest integer.

For q_{OCL}^{σ}, q_{LCL}^{σ}, q_{FDA}^{σ}, and q_{OFL}^{σ}, which range from 0 to 1, Formula (2) shall be used for mapping to yield Q_{OCL}^{σ}, Q_{LCL}^{σ}, Q_{FDA}^{σ}, and Q_{OFL}^{σ}, respectively. For q_{RVU}^{σ}, Formula (48) shall be used for mapping to yield Q_{RVU}^{σ}:

$$Q_{\text{RVU}}^{\sigma} = \left\lfloor 100 \cdot \text{sigmoid}\left(q_{\text{RVU}}^{\sigma}, 1, \frac{1}{2} \right) + \frac{1}{2} \right\rfloor \tag{48}$$

6.2.16.4 Histogram of local quality

Local quality values from orientation certainty (6.2.2), local clarity (6.2.3), frequency domain analysis (6.2.4), ridge valley uniformity (6.2.5) and orientation flow (6.2.6) shall be represented as fixed-length histograms with 10 bins to capture the distribution of local qualities.

The boundaries defining each bin for each of the features are specified as shown in Formula (49):

$$B_{\text{FDA}} = \{-\infty; 0{,}268; 0{,}304; 0{,}33; 0{,}355; 0{,}38; 0{,}407; 0{,}440; 0{,}5; 1; \infty\}$$

$$B_{\text{LCL}} = \{-\infty; 0; 0{,}7; 0{,}740; 0{,}77; 0{,}79; 0{,}81; 0{,}83; 0{,}85; 0{,}87; \infty\}$$

$$B_{\text{OCL}} = \{-\infty; 0{,}337; 0{,}479; 0{,}579; 0{,}655; 0{,}716; 0{,}766; 0{,}81; 0{,}852; 0{,}898; \infty\} \tag{49}$$

$$B_{\text{OFL}} = \{-\infty; 0{,}017\,15; 0{,}035; 0{,}055\,70; 0{,}081; 0{,}115; 0{,}171\,80; 0{,}256\,90; 0{,}475\,80; 0{,}748; \infty\}$$

$$B_{\text{RVU}} = \{-\infty; 0{,}5; 0{,}667; 0; 1; 1{,}25; 1{,}5; 2; 24; 30; \infty\}$$

For each of FDA, LCL, OCL, OFL and RVU, a histogram is computed using the specified bin boundaries where the i-th bin in the histogram is given by the interval shown in Formula (50):

$$\left(B_Q^i, B_Q^{i+1} \right), \qquad \text{for } 1 = i$$

$$B_Q^i, B_Q^{i+1} \right), \qquad \text{for } 1 < i \leq |B_Q| \tag{50}$$

where B_Q is B_{FDA}, B_{LCL}, B_{OCL}, B_{OFL}, or B_{RVU}.

The histograms of local qualities are specified according to their bin boundaries as defined in Formulae (51) and (52) where the i-th bin in the histogram contains the cardinality of the multiset that contains values bounded by the histogram boundaries.

$$q_{\text{FDA}}^i = \left| \left\{ B_{\text{FDA}}^i \leq q_{\text{FDA}}^{\text{local}} < B_{\text{FDA}}^{i+1} \right\} \right|, \text{for } 1 \leq i \leq |B_{\text{FDA}}|,$$

$$q_{\text{LCL}}^i = \left| \left\{ B_{\text{LCL}}^i \leq q_{\text{LCL}}^{\text{local}} < B_{\text{LCL}}^{i+1} \right\} \right|, \text{for } 1 \leq i \leq |B_{\text{LCL}}|,$$

$$q_{\text{OCL}}^i = \left| \left\{ B_{\text{OCL}}^i \leq q_{\text{OCL}}^{\text{local}} < B_{\text{OCL}}^{i+1} \right\} \right|, \text{for } 1 \leq i \leq |B_{\text{OCL}}|, \tag{51}$$

$$q_{\text{OFL}}^i = \left| \left\{ B_{\text{OFL}}^i \leq q_{\text{OFL}}^{\text{local}} < B_{\text{OFL}}^{i+1} \right\} \right|, \text{for } 1 \leq i \leq |B_{\text{OFL}}|,$$

$$q_{\text{RVU}}^i = \left| \left\{ B_{\text{RVU}}^i \leq q_{\text{RVU}}^{\text{local}} < B_{\text{RVU}}^{i+1} \right\} \right|, \text{for } 1 \leq i \leq |B_{\text{RVU}}|.$$

The histogram for a single feature represented by its bins is written as:

$$q_{\text{FDA}} = \left\{ q_{\text{FDA}}^i \right\}, \text{for } 1 \leq i < |B_{\text{FDA}}|,$$

$$q_{\text{LCL}} = \left\{ q_{\text{LCL}}^i \right\}, \text{for } 1 \leq i < |B_{\text{LCL}}|,$$

$$q_{\text{OCL}} = \left\{ q_{\text{OCL}}^i \right\}, \text{for } 1 \leq i < |B_{\text{OCL}}|, \tag{52}$$

$$q_{\text{OFL}} = \left\{ q_{\text{OFL}}^i \right\}, \text{for } 1 \leq i < |B_{\text{OFL}}|,$$

$$q_{\text{RVU}} = \left\{ q_{\text{RVU}}^i \right\}, \text{for } 1 \leq i < |B_{\text{RVU}}|.$$

6.2.16.5 ISO/IEC 29794-4 quality feature vector

The quality feature vector that is input to the unified quality score computation (see 6.4) is specified as shown in Formula (53):

$$
\begin{aligned}
Q_{29794\text{-}4} = \{ & q_{\text{OCL}}^{\mu}, \quad q_{\text{LCL}}^{\mu}, \quad q_{\text{FDA}}^{\mu}, \quad q_{\text{RVU}}^{\mu}, \quad q_{\text{OFL}}^{\mu}, \\
& q_{\text{OCL}}^{\sigma}, \quad q_{\text{LCL}}^{\sigma}, \quad q_{\text{FDA}}^{\sigma}, \quad q_{\text{RVU}}^{\sigma}, \quad q_{\text{OFL}}^{\sigma}, \\
& q_{\text{OCL}}, \quad q_{\text{FDA}}, \quad q_{\text{LCL}}, \quad q_{\text{RVU}}, \quad q_{\text{OFL}}, \\
& q_{\text{MU}}, \quad q_{\text{MMB}}, \quad q_{\text{COH}}^{\text{REL}}, \quad q_{\text{COH}}^{\text{sum}}, \quad q_{\text{AREA}}^{\mu}, \\
& q_{\text{MIN}}^{\text{CNT}}, \quad q_{\text{MIN}}^{\text{COM}}, \quad q_{\text{MIN}}^{\text{MU}}, \quad q_{\text{MIN}}^{\text{OCL}} \}
\end{aligned}
\tag{53}
$$

6.3 Non-normative quality measures

6.3.1 General

Subclause 6.3 specifies algorithms for computing further finger image quality components, which, however, are not used in the computation of the unified quality score.

6.3.2 Radial power spectrum

6.3.2.1 Description

The radial power spectrum is a measure of maximal signal power in a defined frequency band of the global radial Fourier spectrum. Ridges can be locally approximated by means of a single sine wave, hence high energy concentration in a narrow frequency band corresponds to consistent ridge structures.

Since the ridges of a finger image can be locally approximated by one sine wave, large values of sine wave energy can represent strong ridges. The robustness of the ridge structure can be used to measure finger image quality. $\dot{F}$ is decided as the maximum Radial Fourier spectrum value within the reasonable Fourier domain. The reasonable Fourier domain refers to the region of neither the highest nor the lowest frequency. The higher the value of $\dot{F}$, the better the finger image quality.

6.3.2.2 Variables

Name	Default	Description
r_{min}	0,143 cycles/pixel	Lower bound of frequency band
r_{max}	0,077 cycles/pixel	Upper bound of frequency band
Δ_r	1 pixel	Sampling step between annular bands in the frequency spectrum
θ	180	Degrees of the spectrum to consider

6.3.2.3 Algorithm

a) Compute the magnitude of the 2D-DFT $\dot{F}(u,v)$ of input image, discarding the DC component.

b) Transform $\dot{F}(u,v)$ into polar coordinates and normalize to the range of $[0,1]$.

c) Determine the maximum energy (i.e. the maximum magnitude of all frequencies) to compute Q_{POW} (6.3.2.5).

6.3.2.4 Magnitude of frequency bands polar coordinates

J, the magnitude of the annular band between r and $r+\Delta_r$ in the polar Fourier spectrum $\dot{F}(\alpha,r)$, is computed as shown in Formula (54):

$$J(r) = \frac{\sum_{\alpha=0}^{\pi}\sum_{r}^{r+\Delta_r}\dot{F}(\alpha,r)}{\sum_{\alpha=0}^{\pi}\sum_{r_{min}}^{r_{max}}\dot{F}(\alpha,r)} \tag{54}$$

where

α is the angle;

r is the radius.

$\dot{F}(\alpha,r)$ is the Spectrum $f(p,q)$ representation in polar coordinate system (α,r), see Figure 9.

| a) Fourier spectrum of input | b) Fourier spectrum in polar coordinate system | c) View of frequencies of interest | d) 1D magnitude of frequencies of interest |
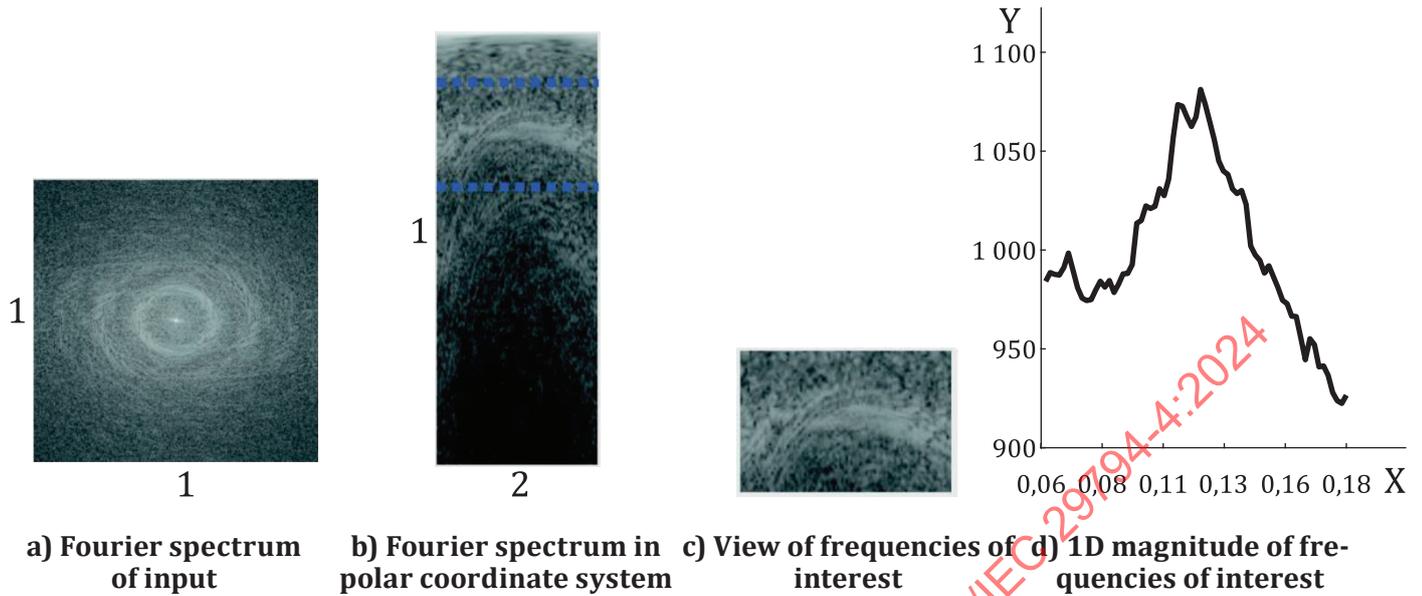
Key

X   cycles/pixel

Y   magnitude

1   cycles/pixel

2   radians

Figure 9 — Processing steps of radial power spectrum algorithm

6.3.2.5   Determine quality from energy distribution

The quality feature q_{POW} is found as shown in Formula (55):

$$q_{POW} = \max_{r \in [\Delta r]} |J(r)| \tag{55}$$

NOTE   The radial power spectrum depends on the spatial sampling rate. The given defaults assume 196,85 pixels per centimetre (500 pixels per inch).

6.3.3   Gabor filter bank

6.3.3.1   Feature description

The Gabor quality feature operates on a per-pixel basis by calculating the standard deviation of the Gabor filter bank responses.[10] The size of the filter bank is used to determine a number of filters oriented evenly across the half circle. The strength of the response at a given location corresponds to the agreement between filter orientation and frequency in the location neighbourhood. For areas in the fingerprint image with a regular ridge-valley pattern there will be a high response from one or a few filter orientations. In areas containing background or unclear ridge-valley structure the Gabor response of all orientations will be low and constant.

6.3.3.2 Variables

Name	Default	Description
σ_x	6	2D Gaussian standard deviation in x-direction
σ_y	6	2D Gaussian standard deviation in y-direction
n	4	Size of filter bank (orientations of the Gabor wave)
f	0,1	Gabor filter frequency
θ	—	An orientation of a Gabor filter

6.3.3.3 Algorithm

a) Convolve input image with a 2D Gaussian kernel with $\sigma = 1$ and subtract it from the input image I to give $\tilde{I}$.

b) Compute the Gabor response of $\tilde{I}$ for each orientation θ.

c) Convolve the magnitude (complex modulus) of each Gabor response with a 2D Gaussian kernel with $\sigma = 4$.

d) Compute the standard deviation of the Gabor magnitude response values at each location yielding a map of standard deviations.

e) Sum the map of standard deviations and normalize according to number of sample points to produce the final Gabor quality.

Figure 10 visualizes the processing steps.

6.3.3.4 Gabor filter

The general form of the complex 2D Gabor[11] filter, h_{Cx}, in the spatial domain is given by Formula (56):

$$h_{Cx}\left(x,y;f,\theta,\sigma_x,\sigma_y\right) = \exp\left(-\frac{1}{2}\left(\frac{x_\theta^2}{\sigma_x^2} + \frac{y_\theta^2}{\sigma_y^2}\right)\exp\left(j2\pi f x_\theta\right)\right) \tag{56}$$

where x_θ and y_θ are calculated using Formulae (57) and (58) respectively:

$$x_\theta = x\sin\theta + y\cos\theta \tag{57}$$

$$y_\theta = x\cos\theta - y\sin\theta \tag{58}$$

and f is the frequency (cycles/pixel) of the sinusoidal plane wave along the orientation θ. The size of the Gaussian smoothing window is determined by σ_x, σ_y.

The filter bank size n is used to compute the differently oriented Gabor filters composing the filter bank. Computing θ given n is done as shown in Formula (59):

$$\theta = \frac{k-1}{n\pi}, k = 1,\ldots,n \tag{59}$$

NOTE   The Gabor quality feature is spatial sampling rate dependent. The given defaults assume 196,85 pixels per centimetre (500 pixels per inch).

6.3.3.5 Computing the Gabor quality from the Gabor filter response

Let G be a matrix with standard deviations of local responses resulting from convolution of I and Gabor filter of orientation n. The Gabor quality q_{GAB} is computed as shown in Formula (60):

$$q_{GAB} = \frac{1}{X \times Y} \sum_x \sum_y G(x,y) \tag{60}$$

a) Resulting image $\hat{I}$ **b) Real valued Gabor filter** h **c) Gabor filter** h

d) $\hat{I}$ **convolved with** h **yielding matrix of filter responses** G_0 **e)** G_0 **convolved with 2D Gaussian kernel** **f) Standard deviation of filter responses at each pixel**
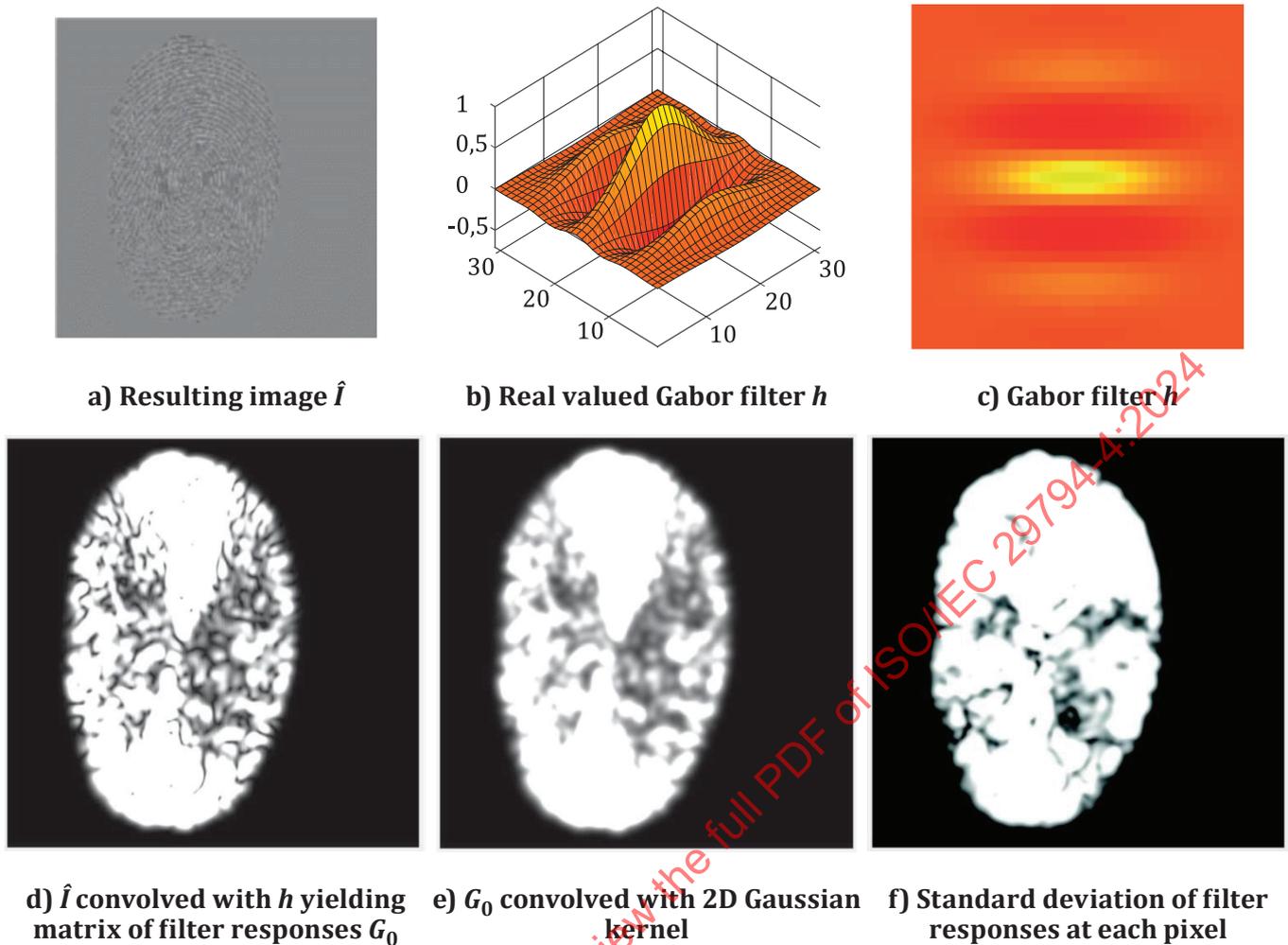
Figure 10 — Processing steps of Gabor algorithm

6.4 Unified quality score

6.4.1 Methodology for combining quality components

In order to obtain a single or unified output from several quality components described in the earlier clauses, it is necessary to combine those values to produce a single scalar quality score as required in the quality field of ISO/IEC 29794-1. Combining quality components shall be done such that the overall quality score is predictive of performance. There are various methods that can be used to combine quality components, e.g. weighted averaging, the use of pattern classifiers and other nonlinear computations.

6.4.2 Training method

Pattern classifiers are mathematical models that can intelligently learn a concept and predict an output when presented with new and even unseen samples. To apply pattern classification to combine the finger image quality analysis measures, it is necessary to train the pattern classifier by providing the values for the quality measures computed for training samples, along with the ground-truth classification [described in a) and b) below] for each of these samples. Once the pattern classifier is well-trained, given the values of the quality measures, it will be able to provide an overall quality score for the finger image.

The feature vector, $Q_{29794\text{-}4}$ (6.2.16.5), shall be the input to the pattern classifier. Training the pattern classifier can be performed using a corpus of finger images with pre-assigned quality categories or scores such as the QSND corpus, on the output of one or many quality algorithms. For all the samples in the corpus,

the feature vectors are computed. They are then paired with the quality category or score and fed into the pattern classifier for training.

With the feature vector specified in 6.2.16.5, a random forest shall be trained for binary classification, where Class 0 represents images of very low utility and Class 1 represents images of very high utility. The trained random forest outputs class membership along with its probability score. This score is the probability that a given image belongs to class 1 multiplied by 100 and rounded to its closest integer.

The training set shall be chosen such that:

a) class 1 (or high utility) consists of images with NFIQ 1.0[12] value of 1 (with activation score > 0,7) and mated similarity score in the 90th percentile for each of the comparison score providers;

b) class 0 (or low utility) consists of images with NFIQ 1.0 value of 5 (with activation score > 0,9) and mated similarity score smaller than a decision threshold value that corresponds to false match rate of 1 in 10 000, i.e. false reject at false match rate of 0,000 1.

7 Finger image quality block

7.1 Binary encoding

In binary biometric data blocks, quality data should be encoded as specified in ISO/IEC 39794-1.

Quality measures for finger images encoded in the format specified in ISO/IEC 39794-4 should be placed into the quality blocks of that format. CBEFF quality fields should not be used in place of ISO/IEC 39794-4 quality fields but rather as supplementary data. The prescribed use of CBEFF quality fields may be supplied by each CBEFF patron format standard and is beyond the scope of this document. Multiple quality measures calculated by the same algorithm (i.e. same quality algorithm vendor identifier and same quality algorithm identifier) shall not be present in a single biometric data interchange record.

7.2 XML encoding

In XML documents, quality data shall be encoded as specified in ISO/IEC 39794-1.

7.3 Quality algorithm identifiers

The owner of the quality algorithms defined in this document is ISO/IEC JTC 1/SC 37. Its organization identifier is 257 (101_{Hex}). Table 1 lists the quality algorithm identifiers for the quality measures defined in this document, which have been registered in accordance with ISO/IEC 19785-2 to identify the quality measures defined in this document.

The biometric organization identifier of ISO/IEC JTC 1/SC 37 shall be used as the quality algorithm vendor identifier if and only if a reference implementation approved by ISO/IEC JTC 1/SC 37 is used to compute the quality score. An approved reference implementation is posted at Reference [16].

If a unified quality score is calculated and reported in a finger image quality block, the normative quality measures defined in 6.2 should be calculated first. The values of the normative quality components defined in 6.2 may be reported in the finger image quality block, but this is not mandatory. Calculation of the non-normative quality components defined in 6.3 is optional. Their values cannot be reported in an ISO/IEC 29794-1 quality block because they are not mapped to integers in the range 0 to 100.

NOTE 1   The unified quality score summarizes the quality components in Formula (53) in 6.2.16.5.

NOTE 2   Revisions to the reference implementation NFIQ 2 have corrected software defects which calculated the unified quality score incorrectly. Tagged revisions to this reference implementation are listed in Table 1.

Table 1 — Quality algorithm identifiers

Quality algorithm identifier Hex	Quality algorithm identifier decimal	Description	Symbol	Governing subclause
21_{Hex}	33	Unified quality score, reference implementation NFIQ 2 tag v2.0.0	$Q_{NFIQ2\ v2.0.0}$	6.4
22_{Hex}	34	Mean of local orientation certainty level	Q_{OCL}^{μ}	6.2.16.2.2
23_{Hex}	35	Standard deviation of local orientation certainty level	Q_{OCL}^{σ}	6.2.16.3.2
24_{Hex}	36	Mean of local clarity	Q_{LCL}^{μ}	6.2.16.2.2
25_{Hex}	37	Standard deviation of local clarity	Q_{LCL}^{σ}	6.2.16.3.2
26_{Hex}	38	Mean of local frequency domain analysis	Q_{FDA}^{μ}	6.2.16.2.2
27_{Hex}	39	Standard deviation of local frequency domain analysis	Q_{FDA}^{σ}	6.2.16.3.2
28_{Hex}	40	Mean of local ridge valley uniformity	Q_{RVU}^{μ}	6.2.16.2.2
29_{Hex}	41	Standard deviation of local ridge valley uniformity	Q_{RVU}^{σ}	6.2.16.3.2
$2A_{Hex}$	42	Mean of local orientation flow	Q_{OFL}^{μ}	6.2.16.2.2
$2B_{Hex}$	43	Standard deviation of orientation flow	Q_{OFL}^{σ}	6.2.16.3.2
$2C_{Hex}$	44	MU	Q_{MU}	6.2.7.3
$2D_{Hex}$	45	MMB	Q_{MMB}	6.2.8.3
$2E_{Hex}$	46	Minutiae count	Q_{MIN}^{CNT}	6.2.9.3
$2F_{Hex}$	47	Minutiae count in centre of mass	Q_{MIN}^{COM}	6.2.10.3
30_{Hex}	48	Minutiae quality based on image mean	Q_{MIN}^{MU}	6.2.11.3
31_{Hex}	49	Minutiae quality based on orientation certainty level	Q_{MIN}^{OCL}	6.2.12.3
32_{Hex}	50	Region of interest image mean	Q_{AREA}^{μ}	6.2.13.4
33_{Hex}	51	Region of interest orientation map coherence sum	Q_{COH}^{sum}	6.2.14.5
34_{Hex}	52	Region of interest relative orientation map coherence sum	Q_{COH}^{REL}	6.2.15.3
35_{Hex}	53	*Reserved for future use*		
36_{Hex}	54	*Reserved for future use*		
37_{Hex}	55	Unified quality score, reference implementation NFIQ 2 tag v2.1.0	$Q_{NFIQ2\ v2.1.0}$	6.4
38_{Hex}	56	Unified quality score, reference implementation NFIQ 2 tag v2.2.0	$Q_{NFIQ2\ v2.2.0}$	6.4
39_{Hex}	57	Unified quality score, reference implementation NFIQ 2 tag v2.3.0	$Q_{NFIQ2\ v2.3.0}$	6.4
$3A_{Hex}$–40_{Hex}	58–64	*Reserved for future use*		

Annex A
(normative)

Conformance test assertions

A.1 Overview

In order to achieve the objective of this document, it is necessary to test biometric products to ensure their conformance. Conformant implementations are a necessary prerequisite for achieving interoperability among implementations. Therefore, there is a need for a standardized conformance testing methodology, test assertions and test procedures as applicable to specific modalities addressed by this document. The test assertions cover all normative contributive quality components, so that the conformity results produced by the test suites will reflect the real degree of conformity of the implementations to ISO/IEC 29794-4 finger image quality blocks.

This annex specifies conformance test criteria and a conformance test set to determine whether any implementation claiming conformance to this document conforms to the reference implementation NFIQ 2.

A.2 Conformance test set

To verify conformance, implementations of quality assessment algorithms claiming conformance with this document should run on all images in the conformance test set. In order to conform, the absolute value of the difference between the computed output value and the target unified quality score $Q_{\text{NFIQ2 v2.3.0}}$ in Table A.1 shall not be more than 1 (i.e. 1 % of the maximum value 100). The contents of Table A.1 are available in comma-separated values format from Reference [15]. The values of Table A.1 mapped 0-100 to fit into a quality block as specified in ISO/IEC 29794-1 are shown in Table A.2, which is also available in comma-separated values format from the same location.

The finger images in the conformance test set are selected from databases from the National Institute of Standards and Technology entitled Special Database 300[13] and Special Database 302.[14] The conformance test set can be requested from Reference [15].

NFIQ 2, the source code of which is available from Reference [16], is a reference implementation for this document. The pre-compiled release of version 2.3.0 of this reference implementation produces no differences from the values in Table A.1 and Table A.2.

Table A.1 — Target quality measure values for conformance test set

Identifier	$Q_{NFIQ2\ v2.3.0}$	q_{FDA}^{μ}	q_{FDA}^{σ}	q_{MIN}^{COM}	q_{MIN}^{CNT}	q_{MIN}^{MU}	q_{MIN}^{OCL}	q_{AREA}^{μ}	q_{LCL}^{μ}	q_{LCL}^{σ}	q_{MMB}	q_{MU}	q_{OCL}^{μ}	q_{OCL}^{σ}	q_{OFL}^{μ}	q_{OFL}^{σ}	q_{COH}^{REL}	q_{COH}^{sum}	q_{RVU}^{μ}	q_{RVU}^{σ}
00001052_plain_500_10	NA	NA	NA	NA	NA	NA	NA	NA	NA	NA	NA	NA	NA	NA	NA	NA	NA	NA	NA	NA
00001057_plain_500_03	90	0,463 32	0,199 44	32	55	0,327 27	0,709 09	144,924 44	0,809 47	0,169 21	164,344 8	163,218 3	0,823 69	0,150 01	0,319 42	0,297 81	0,701 99	83,537 43	1,116 62	0,809 59
00001308_plain_500_08	68	0,484 27	0,200 02	16	44	0,431 81	0,590 90	161,906 96	0,808 12	0,211 51	180,626 8	179,957 4	0,776 32	0,152 70	0,184 06	0,226 64	0,691 81	88,551 78	1,143 47	0,654 04
00001428_plain_500_07	76	0,557 55	0,260 46	31	88	0,261 36	0,295 45	167,289 85	0,761 09	0,241 69	185,912 0	184,928 9	0,751 32	0,169 34	0,355 75	0,356 01	0,614 64	70,069 32	1,143 28	0,850 57
00001610_plain_500_10	12	0,641 90	0,331 30	149	189	0,417 98	0,031 74	160,571 34	0,621 38	0,281 23	179,685 7	177,541 5	0,598 00	0,219 88	0,268 39	0,237 78	0,474 84	51,758 05	1,306 79	1,040 58
00001655_plain_500_04	39	0,469 04	0,260 95	89	147	0,136 95	0,027 21	157,981 14	0,723 24	0,219 17	183,894 9	182,441 8	0,639 19	0,174 25	0,315 25	0,353 09	0,526 51	75,291 37	1,206 79	0,947 92
00001665_plain_500_08	4	0,588 50	0,336 70	76	192	0,322 91	0,000 00	162,107 97	0,636 12	0,269 49	182,571 8	178,355 9	0,549 24	0,177 12	0,341 58	0,349 34	0,381 28	50,329 59	1,302 55	1,104 72
00001723_plain_500_05	56	0,563 47	0,294 84	30	57	0,210 52	0,056 14	148,064 01	0,625 86	0,348 42	173,630 7	170,416 4	0,737 52	0,184 16	0,282 37	0,289 60	0,658 78	61,267 12	1,201 38	1,029 67
00001880_plain_500_10	4	0,679 52	0,344 09	126	139	0,071 94	0,021 58	228,760 82	0,551 92	0,331 58	166,315 7	159,544 8	0,593 72	0,202 79	0,446 70	0,288 57	0,442 04	33,595 33	1,551 33	1,442 46
00002302_N_500_palm_10	21	0,538 61	0,294 13	79	95	0,431 57	0,000 00	168,144 49	0,636 48	0,244 32	195,682 2	188,512 8	0,490 44	0,176 42	0,354 47	0,277 60	0,350 88	23,860 29	1,097 05	0,757 18
00002302_N_500_palm_10-core	20	0,385 97	0,188 51	42	42	0,500 00	0,000 00	151,182 40	0,646 67	0,199 94	164,357 2	158,231 2	0,420 74	0,170 77	0,351 83	0,034 62	0,308 08	5,545 44	1,195 46	1,106 64
00002304_R_500_slap_01	92	0,427 95	0,168 51	36	122	0,336 06	0,393 44	170,452 38	0,699 12	0,295 96	203,153 7	200,842 2	0,723 43	0,206 64	0,339 20	0,350 95	0,659 46	87,709 16	1,087 26	0,545 64
00002304_R_500_slap_08	31	0,434 30	0,221 52	61	117	0,452 99	0,034 18	172,139 85	0,697 34	0,210 92	197,780 8	195,593 9	0,557 03	0,206 55	0,348 40	0,476 77	0,436 27	30,975 19	1,134 86	1,037 72
00002310_R_500_slap_05	43	0,411 91	0,240 05	63	102	0,470 58	0,107 84	139,712 62	0,672 34	0,251 73	175,390 5	168,578 4	0,656 03	0,193 54	0,286 93	0,254 65	0,502 90	38,723 81	1,084 45	0,603 60
00002314_R_500_slap_01	88	0,449 30	0,176 02	31	65	0,538 46	0,061 53	182,084 25	0,751 96	0,222 58	205,687 4	208,327 6	0,618 94	0,156 00	0,388 26	0,377 85	0,486 36	64,686 58	1,132 77	0,680 04
00002315_R_500_slap_05	3	0,512 71	0,318 45	160	194	0,603 09	0,000 00	165,131 64	0,599 62	0,257 92	190,255 8	183,072 2	0,716 12	0,211 15	0,422 23	0,294 54	0,322 05	25,120 05	1,255 39	0,945 04
00002315_R_500_slap_06	77	0,426 30	0,191 11	53	167	0,437 12	0,149 70	154,464 74	0,754 26	0,170 61	181,857 0	176,641 8	0,719 14	0,167 05	0,351 18	0,360 34	0,578 95	94,949 16	1,098 45	0,568 24
00002317_R_500_slap_01	93	0,450 46	0,135 03	31	101	0,732 67	0,267 32	157,765 41	0,804 73	0,143 86	186,808 6	180,155 4	0,699 27	0,164 66	0,365 07	0,339 37	0,552 76	100,602 46	1,080 25	0,583 93
00002319_R_500_slap_04	57	0,416 80	0,166 56	57	83	0,578 31	0,024 09	190,588 26	0,551 87	0,367 72	203,360 5	202,140 9	0,596 19	0,145 46	0,495 25	0,444 51	0,423 94	34,339 88	1,068 92	0,567 02
00002319_R_500_slap_09	68	0,425 72	0,165 13	37	92	0,652 17	0,000 00	191,283 63	0,597 28	0,316 63	213,879 1	210,579 0	0,530 51	0,155 19	0,471 02	0,367 95	0,404 71	42,494 51	1,059 33	0,502 13
00002319_R_500_slap_10	42	0,456 04	0,185 62	25	44	0,727 27	0,022 72	182,774 80	0,746 70	0,214 13	208,544 3	205,425 9	0,627 70	0,143 09	0,131 11	0,173 42	0,497 49	35,819 41	1,098 49	0,423 06

Table A.1 *(continued)*

Identifier	$O_{NFIQ2\ v2.3.0}$	q^{μ}_{FDA}	q^{σ}_{FDA}	q^{COM}_{MIN}	q^{CNT}_{MIN}	q^{MU}_{MIN}	q^{OCL}_{MIN}	q^{μ}_{AREA}	q^{μ}_{LCL}	q^{σ}_{LCL}	q_{MMB}	q_{MU}	q^{μ}_{OCL}	q^{σ}_{OCL}	q^{μ}_{OFL}	q^{σ}_{OFL}	q^{REL}_{COH}	q^{sum}_{COH}	q^{μ}_{RVU}	q^{σ}_{RVU}
00002320_R_500_slap_06	47	0,428 58	0,247 71	19	177	0,299 43	0,124 29	145,436 82	0,718 15	0,182 11	166,167 9	161,969 2	0,652 48	0,175 32	0,289 54	0,307 65	0,492 43	82,236 27	1,274 33	0,971 02
00002320_R_500_slap_08	7	0,456 79	0,296 90	117	206	0,373 78	0,009 70	158,419 36	0,610 32	0,265 88	170,962 8	171,341 6	0,550 29	0,186 90	0,370 24	0,363 15	0,404 40	44,888 46	1,409 71	1,302 82
00002321_R_500_slap_07	21	0,454 36	0,282 05	105	170	0,570 58	0,035 29	189,221 52	0,638 72	0,249 81	207,202 9	200,814 0	0,525 74	0,200 88	0,393 63	0,311 68	0,369 80	32,542 91	1,334 93	1,106 49
00002325_R_500_slap_04	22	0,435 26	0,255 87	72	133	0,233 08	0,022 55	136,812 72	0,673 83	0,231 28	166,048 5	163,957 4	0,577 59	0,157 29	0,395 43	0,334 61	0,420 09	40,328 60	1,082 47	0,891 45
00002325_R_500_slap_08	31	0,451 22	0,272 64	67	141	0,177 30	0,070 92	130,352 63	0,632 10	0,266 75	166,039 9	160,507 5	0,589 83	0,194 91	0,357 36	0,301 69	0,443 01	45,187 92	1,392 76	1,328 70
00002326_R_500_slap_02	89	0,426 14	0,172 53	34	120	0,408 30	0,075 00	172,351 30	0,780 10	0,142 03	196,784 1	192,845 7	0,707 93	0,163 66	0,254 38	0,261 19	0,541 89	73,698 23	1,177 19	0,692 88
00002326_R_500_slap_05	1	0,464 10	0,301 97	146	240	0,425 00	0,008 33	183,400 61	0,575 26	0,301 77	204,055 6	202,235 6	0,541 35	0,183 74	0,397 89	0,345 13	0,382 22	37,075 60	1,283 63	0,976 83
00002330_R_500_slap_04	49	0,406 40	0,202 11	67	102	0,647 05	0,098 03	163,811 29	0,618 77	0,303 73	187,095 8	182,586 6	0,615 44	0,172 34	0,301 86	0,318 09	0,461 01	43,796 08	1,191 45	0,654 15
00002334_R_500_slap_05	29	0,400 60	0,242 49	80	89	0,528 09	0,123 59	144,662 30	0,638 30	0,278 80	171,226 1	164,490 4	0,731 71	0,134 36	0,227 58	0,244 35	0,551 58	34,198 25	1,229 02	0,860 13
00002334_R_500_slap_07	83	0,422 82	0,174 12	46	82	0,634 14	0,243 90	162,140 06	0,689 94	0,286 22	192,876 6	185,905 8	0,733 60	0,169 96	0,365 31	0,310 07	0,577 86	54,319 70	1,096 65	0,517 55
00002340_R_500_slap_08	28	0,393 78	0,252 25	98	147	0,578 23	0,020 40	195,318 62	0,490 02	0,335 50	209,227 4	208,605 5	0,587 43	0,176 32	0,398 12	0,348 01	0,425 23	35,719 37	1,227 60	0,824 27
00002342_R_500_slap_05	5	0,509 47	0,341 14	184	236	0,461 86	0,000 00	162,252 77	0,538 38	0,313 90	187,167 2	182,843 9	0,576 35	0,146 74	0,168 68	0,196 65	0,410 20	36,918 30	1,472 06	1,228 52
00002342_R_500_slap_09	16	0,425 96	0,291 97	79	154	0,383 11	0,006 49	162,207 80	0,641 34	0,256 34	191,799 3	188,802 5	0,532 86	0,205 65	0,173 50	0,205 98	0,422 36	46,882 84	1,307 87	1,128 23
00002349_N_500_palm_05	26	0,445 14	0,257 64	63	101	0,504 95	0,000 00	105,338 09	0,743 23	0,140 73	147,917 7	141,927 1	0,604 14	0,178 44	0,172 62	0,204 75	0,454 47	40,902 26	1,201 63	0,822 10
00002349_R_500_slap_07	13	0,467 34	0,279 42	99	152	0,519 73	0,019 73	133,314 49	0,675 65	0,218 82	164,781 4	160,877 6	0,570 54	0,151 22	0,347 48	0,314 67	0,427 79	35,934 63	1,261 74	1,043 22
00002352_R_500_slap_01	85	0,472 95	0,177 76	24	99	0,767 67	0,424 24	149,140 17	0,780 90	0,232 45	183,105 2	173,996 9	0,792 22	0,133 22	0,324 66	0,355 80	0,678 75	114,709 67	1,097 00	0,645 07
00002352_R_500_slap_10	50	0,395 73	0,215 89	45	78	0,717 94	0,064 10	184,677 67	0,689 34	0,212 55	204,841 8	201,127 5	0,602 61	0,151 47	0,280 07	0,278 31	0,452 70	42,101 46	1,345 00	0,938 40
00002353_N_500_palm_10	39	0,459 46	0,270 86	79	134	0,417 91	0,425 37	146,797 00	0,405 17	0,395 10	187,993 5	179,268 6	0,750 06	0,204 17	0,310 80	0,315 36	0,643 51	49,550 72	1,192 08	0,741 33
00002353_R_500_slap_06	48	0,408 21	0,183 06	60	183	0,306 01	0,579 23	128,025 55	0,504 04	0,381 99	165,425 0	161,483 4	0,831 12	0,144 86	0,256 66	0,303 83	0,759 77	100,290 13	1,086 93	0,605 78
00002353_R_500_slap_10	35	0,440 50	0,270 35	88	130	0,553 84	0,269 23	182,837 94	0,336 50	0,377 11	213,123 0	208,743 0	0,682 75	0,168 35	0,257 66	0,266 38	0,527 61	41,153 99	1,208 48	1,092 68
00002356_N_500_palm_05	47	0,422 50	0,172 95	52	89	0,337 07	0,022 47	130,134 73	0,806 28	0,052 72	161,387 9	158,511 0	0,700 56	0,127 26	0,396 44	0,367 89	0,534 16	57,689 31	1,396 17	1,328 11

Table A.1 *(continued)*

Identifier	$O_{NFIQ2\ v2.3.0}$	q^μ_{FDA}	q^σ_{FDA}	q^{COM}_{MIN}	q^{CNT}_{MIN}	q^{MU}_{MIN}	q^{OCL}_{MIN}	q^μ_{AREA}	q^μ_{LCL}	q^σ_{LCL}	q_{MMB}	q_{MU}	q^μ_{OCL}	q^σ_{OCL}	q^μ_{OFL}	q^σ_{OFL}	q^{REL}_{COH}	q^{sum}_{COH}	q^μ_{RVU}	q^σ_{RVU}
00002357_R_500_slap_02	86	0,43232	0,16451	31	53	0,54717	0,30188	143,47705	0,80190	0,13555	166,6973	163,7842	0,75774	0,13024	0,37613	0,26737	0,60605	59,39376	1,08529	0,59116
00002357_R_500_slap_04	60	0,36192	0,13958	63	96	0,82291	0,23958	117,19903	0,74625	0,19523	144,1611	139,4977	0,76321	0,14243	0,29938	0,26794	0,60815	63,85630	1,16083	0,57848
00002357_R_500_slap_08	44	0,41594	0,21712	97	143	0,61538	0,07692	124,57630	0,71119	0,22460	154,4342	144,7081	0,68957	0,15437	0,37146	0,33608	0,53354	55,48875	1,20359	0,83136
00002358_R_500_slap_05	24	0,42752	0,22324	47	68	0,35294	0,00000	133,27844	0,69111	0,22465	173,7606	165,4071	0,62375	0,14380	0,11837	0,14079	0,46792	36,96607	1,06143	0,64883
00002359_J_500_palm_10	44	0,39863	0,17283	58	105	0,37142	0,07619	134,31180	0,73910	0,20659	163,2521	163,2521	0,60742	0,23142	0,28428	0,25485	0,51346	49,80605	1,19037	0,94461
00002361_R_500_slap_03	47	0,39788	0,18445	78	128	0,69500	0,03906	165,05254	0,65028	0,24456	181,3926	176,9338	0,59523	0,18898	0,28979	0,29030	0,43104	48,27695	1,18200	0,79856
00002362_N_500_palm_05	34	0,53332	0,29189	42	75	0,21333	0,18666	131,47815	0,73821	0,19029	159,3834	157,7113	0,68979	0,17344	0,21771	0,20428	0,54859	45,53303	1,24907	1,06423
00002362_R_500_slap_03	34	0,50776	0,28383	97	124	0,41129	0,06032	183,62964	0,59440	0,33616	204,4770	201,1449	0,62411	0,20615	0,24482	0,25712	0,49344	40,95569	1,34713	1,17365
00002362_R_500_slap_05	31	0,46830	0,26942	64	98	0,47959	0,09183	152,93190	0,66449	0,24899	181,3446	172,6756	0,66096	0,14221	0,24242	0,26419	0,49231	37,41570	1,21145	1,18458
00002362_R_500_slap_09	34	0,45367	0,25067	100	132	0,25000	0,06060	135,49762	0,70934	0,20841	166,3893	159,9462	0,65703	0,21099	0,26101	0,28986	0,53504	52,96941	1,18427	0,75563
00002364_R_500_slap_09	28	0,45211	0,26275	80	124	0,34677	0,04838	144,88302	0,62102	0,29609	169,9758	167,7797	0,56654	0,22304	0,59085	0,32526	0,42871	38,15535	1,12277	0,72587
00002367_R_500_slap_03	50	0,37378	0,13817	37	50	0,68000	0,00000	180,97500	0,73733	0,19381	199,4070	194,7487	0,65196	0,10719	0,38793	0,30393	0,48427	32,93098	1,05582	0,60012
00002368_J_500_palm_10	16	0,45438	0,30270	123	159	0,35849	0,03773	150,55885	0,62226	0,27679	121,0265	167,7420	0,64945	0,15930	0,25861	0,25378	0,49983	38,98740	1,26094	0,87108
00002371_J_500_palm_07	83	0,43749	0,16213	43	78	0,51282	0,39743	155,14987	0,78213	0,15719	182,0241	176,7561	0,76053	0,18560	0,29503	0,30470	0,66031	69,99326	1,08556	0,51590
00002373_R_500_slap_06	94	0,43313	0,16094	34	149	0,28187	0,34228	150,17132	0,75775	0,23192	183,9638	179,1577	0,75267	0,20437	0,36612	0,29513	0,69709	99,68445	1,07524	0,69674
00002374_R_500_slap_10	21	0,50232	0,29005	48	70	0,15714	0,00000	121,70483	0,75013	0,18990	168,5035	163,6173	0,66304	0,13328	0,07089	0,06164	0,45125	29,33178	1,30430	1,11433
00002375_J_500_palm_02	82	0,42963	0,13888	24	49	0,42857	0,55102	196,25108	0,75105	0,25144	208,5436	207,6294	0,80142	0,13539	0,23040	0,25069	0,67443	66,76941	1,12118	0,63284
00002376_R_500_slap_03	85	0,42495	0,16956	25	86	0,48837	0,04651	159,91945	0,74508	0,16841	180,0838	176,3743	0,61329	0,16339	0,26693	0,30382	0,44992	62,98890	1,23875	0,90125
00002376_R_500_slap_05	51	0,46156	0,22698	50	98	0,27551	0,04081	129,03228	0,74550	0,18369	166,8466	156,6081	0,62783	0,19227	0,26336	0,28705	0,47022	58,30821	1,21898	0,92994
00002383_J_500_palm_05	45	0,43139	0,20425	40	75	0,52000	0,06666	179,22749	0,75442	0,15101	196,8928	196,0434	0,66242	0,15231	0,19381	0,23485	0,48435	36,32658	1,20580	0,85998
00002383_R_500_slap_06	91	0,41231	0,12735	29	77	0,50649	0,46753	142,26136	0,81800	0,14916	169,1027	162,4066	0,81219	0,11721	0,27202	0,31624	0,69350	111,65397	1,11160	0,57554

Table A.1 *(continued)*

Identifier	$O_{NFIQ2\ v2.3.0}$	q^μ_{FDA}	q^σ_{FDA}	q^{COM}_{MIN}	q^{CNT}_{MIN}	q^{MU}_{MIN}	q^{OCL}_{MIN}	q^μ_{AREA}	q^μ_{LCL}	q^σ_{LCL}	q_{MMB}	q_{MU}	q^μ_{OCL}	q^σ_{OCL}	q^μ_{OFL}	q^σ_{OFL}	q^{REL}_{COH}	q^{sum}_{COH}	q^μ_{RVU}	q^σ_{RVU}
00002384_N_500_palm_05	6	0,50332	0,30532	105	160	0,30625	0,00000	183,72436	0,60458	0,24426	205,5944	201,8574	0,42794	0,17569	0,37619	0,27417	0,28176	21,69580	1,29181	1,13162
00002384_R_500_slap_04	3	0,52660	0,33714	148	255	0,36078	0,00000	170,21354	0,52471	0,32536	201,3710	198,7211	0,50608	0,18696	0,14919	0,20662	0,35161	34,45825	1,29140	0,90675
00002386_R_500_slap_04	0	0,48639	0,34260	151	255	0,63137	0,00784	159,13266	0,51621	0,31813	180,5913	176,7493	0,50523	0,16610	0,24639	0,24556	0,34240	35,26725	1,36931	1,38298
00002391_R_500_slap_07	31	0,39813	0,23062	120	184	0,58152	0,00000	197,65130	0,67478	0,22362	211,7365	207,9484	0,55895	0,13531	0,42529	0,31782	0,41659	41,65902	1,18921	0,85749
00002392_R_500_slap_04	81	0,43436	0,18714	35	90	0,64444	0,33333	127,11564	0,79053	0,16750	159,1244	149,6036	0,72556	0,19396	0,33971	0,31950	0,58715	75,15548	1,10083	0,65312
00002392_R_500_slap_08	78	0,42184	0,13653	52	97	0,68041	0,24742	149,35746	0,77067	0,19876	169,9044	165,5275	0,70965	0,16315	0,31390	0,30437	0,55376	67,55962	1,11732	0,72755
00002396_R_500_slap_01	38	0,40880	0,23348	96	247	0,58299	0,02429	112,24217	0,66227	0,24596	149,5090	142,0725	0,61483	0,19015	0,27105	0,31176	0,45516	89,66656	1,28496	0,86690
00002396_R_500_slap_08	21	0,37167	0,23341	119	244	0,70491	0,01229	168,99954	0,56818	0,28584	188,5453	182,1515	0,52485	0,19929	0,17027	0,20853	0,37891	41,68005	1,28460	1,03064
00002399_L_500_palm_08	55	0,43852	0,22003	74	107	0,20560	0,17757	179,3705	0,62903	0,28731	204,1594	198,8655	0,70903	0,20238	0,18824	0,23501	0,63841	46,60424	1,22544	0,93026
00002401_N_500_palm_02	67	0,43818	0,16640	19	33	0,39393	0,30303	133,58312	0,80504	0,10926	156,6443	150,5038	0,73576	0,14265	0,38838	0,33835	0,55789	49,65288	1,17304	0,68617
00002401_R_500_slap_06	80	0,40251	0,16144	25	95	0,36842	0,49473	125,04243	0,82091	0,08668	158,3009	150,4467	0,79537	0,17071	0,25024	0,28085	0,67881	107,25346	1,22229	0,71148
00002401_R_500_slap_08	75	0,36141	0,12203	32	59	0,55932	0,18644	158,80871	0,79287	0,06369	174,7662	171,7308	0,69788	0,16890	0,33527	0,31598	0,54012	51,85178	1,14811	0,69503
00002403_R_500_slap_04	30	0,38823	0,22685	87	151	0,45033	0,00000	151,45637	0,66329	0,23329	178,3861	169,6813	0,61028	0,10465	0,18185	0,22871	0,44806	55,11241	1,27531	0,93566
00002405_R_500_slap_01	75	0,45283	0,11609	18	62	0,61290	0,82258	152,04328	0,82509	0,17205	182,0624	176,0032	0,87961	0,09674	0,23011	0,29614	0,79728	126,76894	1,04818	0,40472
00002406_R_500_slap_05	4	0,53636	0,33987	122	156	0,51282	0,00000	134,09743	0,63265	0,25394	163,6829	158,3692	0,61626	0,12953	0,18956	0,16788	0,44520	30,27408	1,38692	1,35278
00002406_R_500_slap_08	9	0,45966	0,30477	156	223	0,50672	0,00896	173,85100	0,59312	0,28303	193,3888	188,5868	0,56367	0,15457	0,21883	0,21107	0,39686	35,32064	1,32195	1,21315
00002408_R_500_slap_02	60	0,38021	0,18121	58	94	0,63829	0,04255	168,96225	0,70743	0,22131	190,0953	186,1817	0,65714	0,13269	0,31839	0,25514	0,49327	43,90138	1,11658	0,73406
00002408_R_500_slap_08	46	0,40921	0,22782	78	99	0,79798	0,04040	173,70748	0,68845	0,22932	190,9610	185,5701	0,64862	0,12910	0,50503	0,32125	0,47740	44,87648	1,23446	0,90198
00002409_R_500_slap_02	63	0,44366	0,21234	37	73	0,36986	0,01369	169,46532	0,73908	0,18122	192,9980	192,5841	0,62894	0,14175	0,27163	0,26594	0,47828	53,08925	1,25979	1,11173
00002409_R_500_slap_09	15	0,46350	0,29885	101	204	0,61764	0,01960	120,63536	0,60217	0,29718	143,3653	140,6675	0,66774	0,18226	0,18174	0,22232	0,50317	57,36204	1,35699	1,03935
00002415_R_500_slap_05	31	0,43100	0,25777	44	77	0,58441	0,12987	122,93578	0,68384	0,19941	156,0232	150,7914	0,63361	0,16944	0,31660	0,38657	0,50096	37,07113	1,14941	0,71762

Table A.1 *(continued)*

Identifier	$O_{NFIQ2\ v2.3.0}$	q_{FDA}^{μ}	q_{FDA}^{σ}	q_{MIN}^{COM}	q_{MIN}^{CNT}	q_{MIN}^{MU}	q_{MIN}^{OCL}	q_{AREA}^{μ}	q_{LCL}^{μ}	q_{LCL}^{σ}	q_{MMB}	q_{MU}	q_{OCL}^{μ}	q_{OCL}^{σ}	q_{OFL}^{μ}	q_{OFL}^{σ}	q_{COH}^{REL}	q_{COH}^{sum}	q_{RVU}^{μ}	q_{RVU}^{σ}
00002415_R_500_slap_09	48	0,40761	0,17935	34	56	0,67857	0,26785	93,88252	0,78432	0,15187	125,2220	119,0138	0,80107	0,13215	0,18777	0,20486	0,67799	56,27333	1,19466	0,82060
00002418_R_500_slap_06	72	0,41827	0,19366	39	133	0,27067	0,24060	116,80202	0,75022	0,20058	152,2198	144,9581	0,75426	0,15257	0,30807	0,31250	0,62369	107,27626	1,23864	0,88033
00002420_R_500_slap_04	63	0,42155	0,19744	51	81	0,41975	0,18518	159,02547	0,67863	0,26970	188,7399	183,4693	0,65817	0,20537	0,27268	0,24330	0,49683	44,71543	1,19652	0,74776
00002420_R_500_slap_09	58	0,40506	0,21166	41	85	0,23529	0,31764	119,81425	0,71332	0,25145	161,2539	152,5190	0,77634	0,13259	0,23545	0,21276	0,61883	60,64619	1,20782	0,72929
00002424_R_500_slap_01	94	0,45153	0,16360	25	83	0,25882	0,24705	165,05791	0,78865	0,17403	192,5942	189,3551	0,69259	0,16970	0,30789	0,29247	0,55127	85,44710	1,08316	0,48997
00002428_R_500_slap_02	93	0,44693	0,14566	31	67	0,41746	0,50746	158,13936	0,82180	0,13588	186,3723	179,1480	0,77129	0,18472	0,28613	0,27081	0,66286	69,60033	1,03949	0,54110
00002433_J_500_palm_08	94	0,43928	0,14324	24	62	0,58064	0,58064	164,81934	0,76580	0,21999	187,8390	179,1216	0,76993	0,18130	0,23320	0,26743	0,67784	89,47583	1,10119	0,57288
00002433_J_500_palm_09	86	0,44922	0,15016	30	83	0,30120	0,54216	144,68716	0,80092	0,15619	175,6594	168,9419	0,73954	0,23042	0,23874	0,25609	0,66424	96,31535	1,09520	0,49230
00002433_N_500_palm_07	84	0,43717	0,12525	24	65	0,55384	0,64615	228,56838	0,81117	0,16276	155,6768	151,7523	0,82681	0,13074	0,23210	0,25157	0,70274	93,46528	1,08306	0,44101
00002434_N_500_palm_04	66	0,44140	0,20567	49	77	0,20779	0,23376	155,59872	0,77470	0,15593	186,8055	181,8194	0,70560	0,21422	0,31679	0,33131	0,61025	45,15918	1,12560	0,60398
00002435_N_500_palm_03	82	0,43620	0,15419	27	45	0,44444	0,51111	179,41828	0,70993	0,30101	199,9062	193,7170	0,82553	0,13941	0,26262	0,25695	0,70032	60,92790	1,07311	0,45912
00002437_S_500_slap_08	74	0,43080	0,16331	21	51	0,19607	0,27451	151,04039	0,75602	0,23020	178,1355	172,8261	0,77696	0,09772	0,20989	0,25875	0,64557	63,91168	1,11981	0,60463
00002439_Q_500_palm_02	79	0,41566	0,16113	55	88	0,56818	0,22727	179,82768	0,74334	0,24294	196,5555	193,0141	0,73951	0,10930	0,30038	0,24630	0,57139	59,99668	1,07697	0,44205
00002439_S_500_slap_10	33	0,42845	0,23324	77	97	0,43299	0,00000	180,74923	0,66780	0,22781	203,8171	199,7448	0,57743	0,15672	0,30339	0,23318	0,42998	26,22921	1,27390	0,95476
00002440_R_500_slap_03	94	0,42962	0,14098	34	86	0,80232	0,06976	190,43599	0,77610	0,18743	202,1656	200,5844	0,66553	0,18205	0,28264	0,33628	0,52018	71,78585	1,08283	0,49421
00002443_Q_500_palm_10	55	0,44078	0,20244	28	49	0,40816	0,32653	139,35319	0,78739	0,15764	172,0637	164,2000	0,74094	0,18995	0,15857	0,19296	0,61211	43,46011	1,08914	0,48393
00002445_J_500_palm_02	81	0,47820	0,22178	35	65	0,29230	0,32307	136,47583	0,79150	0,16150	170,6312	160,0127	0,76236	0,17267	0,31760	0,29436	0,65733	69,67761	1,15315	0,58484
00002445_S_500_slap_05	48	0,46344	0,26330	62	90	0,45555	0,10000	90,21601	0,77589	0,13085	124,6426	121,3758	0,73720	0,14477	0,28422	0,28625	0,57555	59,85764	1,24290	0,85994
00002447_R_500_slap_01	38	0,38597	0,22374	94	255	0,65490	0,00784	189,52187	0,60253	0,30460	209,2295	205,2506	0,60091	0,15394	0,34107	0,32076	0,44551	73,06416	1,26793	0,90437
00002447_R_500_slap_06	56	0,38897	0,19529	89	229	0,79039	0,01746	174,96477	0,70883	0,22235	194,2836	190,3706	0,62249	0,17100	0,32441	0,22283	0,46701	79,85965	1,16787	0,87159
00002454_N_500_palm_02	78	0,45444	0,19016	29	69	0,42029	0,30434	146,10713	0,78225	0,16786	172,3074	168,3181	0,74203	0,14355	0,27719	0,25176	0,60864	70,60248	1,22708	1,05187

Table A.1 *(continued)*

Identifier	$O_{NFIQ2\ v2.3.0}$	q^{μ}_{FDA}	q^{σ}_{FDA}	q^{COM}_{MIN}	q^{CNT}_{MIN}	q^{MU}_{MIN}	q^{OCL}_{MIN}	q^{μ}_{AREA}	q^{μ}_{LCL}	q^{σ}_{LCL}	q_{MMB}	q_{MU}	q^{μ}_{OCL}	q^{σ}_{OCL}	q^{μ}_{OFL}	q^{σ}_{OFL}	q^{REL}_{COH}	q^{sum}_{COH}	q^{μ}_{RVU}	q^{σ}_{RVU}
00002455_R_500_slap_01	89	0,44220	0,17815	21	106	0,75471	0,01886	186,41070	0,74555	0,18957	203,2786	199,0101	0,63959	0,13330	0,25400	0,30573	0,47873	85,21512	1,12391	0,59940
00002458_J_500_palm_02	61	0,38966	0,15364	73	122	0,49180	0,00000	180,32171	0,67901	0,26589	196,3432	195,8908	0,65882	0,17380	0,34937	0,28592	0,49757	48,26453	1,06808	0,50615
00002458_N_500_palm_09	19	0,46697	0,27271	149	216	0,44444	0,10185	157,78198	0,49544	0,34576	181,4813	176,4483	0,55360	0,24335	0,35130	0,34513	0,41162	42,80872	1,23290	0,88790
00002458_S_500_slap_02	25	0,47494	0,27820	114	147	0,68707	0,09523	179,95585	0,57876	0,32950	192,1050	192,2906	0,66377	0,19495	0,46592	0,31943	0,50726	42,61017	1,19394	1,08411
00002462_N_500_palm_02	33	0,48683	0,24358	28	63	0,52307	0,04615	169,28443	0,74600	0,14251	198,3099	192,1486	0,56041	0,22886	0,23700	0,23496	0,45620	41,97124	1,36695	1,11515
00002462_R_500_slap_01	89	0,42481	0,15682	29	114	0,34207	0,15789	160,31416	0,78688	0,17010	182,3716	177,9823	0,72055	0,15735	0,26715	0,29658	0,56331	100,83310	1,14424	0,72526
00002462_R_500_slap_03	17	0,45730	0,25135	65	111	0,36036	0,02702	147,50195	0,70351	0,19904	167,2091	165,0457	0,54952	0,18688	0,41838	0,41520	0,37623	38,37562	1,41153	1,14352
00002463_R_500_slap_06	69	0,42800	0,16299	41	90	0,74444	0,00000	167,16686	0,76636	0,10687	188,5580	185,7207	0,60906	0,09120	0,28048	0,29579	0,44378	71,00620	1,15173	0,64266
00002466_N_500_palm_04	77	0,46324	0,18965	29	63	0,19047	0,23809	134,53012	0,78741	0,17459	172,1325	167,3280	0,70881	0,19904	0,42954	0,38642	0,57594	65,65739	1,05488	0,46080
00002475_J_500_palm_04	23	0,41000	0,23825	78	105	0,30476	0,00000	194,39886	0,62045	0,26144	222,0652	219,1824	0,45628	0,15484	0,48713	0,39049	0,32900	18,09549	1,27231	1,08415
00002475_J_500_palm_10	1	0,52961	0,31309	67	101	0,34653	0,00000	190,16986	0,63631	0,22591	215,5463	209,4555	0,42145	0,17073	0,33460	0,23534	0,32349	22,32088	1,36577	1,09775
00002475_S_500_slap_01	10	0,43813	0,28318	86	255	0,48627	0,01568	150,61584	0,59091	0,29718	178,8036	171,1296	0,56481	0,14655	0,28394	0,28816	0,40093	59,73895	1,32990	1,20944
00002475_S_500_slap_04	20	0,38127	0,21356	76	186	0,32258	0,00000	133,44238	0,68756	0,18907	162,8998	154,0480	0,49506	0,15526	0,50348	0,32032	0,32910	33,89778	1,41560	1,33638
00002478_N_500_palm_05	3	0,58618	0,32985	90	144	0,38194	0,05555	140,62484	0,62788	0,24368	183,3071	178,3361	0,53697	0,25109	0,36908	0,33799	0,39474	33,94804	1,42346	1,41254
00002478_Q_500_palm_03	31	0,45201	0,24456	93	156	0,17948	0,08333	151,36919	0,58647	0,31247	173,9627	169,0969	0,60520	0,23465	0,33987	0,34692	0,47444	48,86784	1,18827	0,92244
00002484_Q_500_palm_05	20	0,42390	0,24542	58	66	0,48484	0,07575	161,83316	0,64795	0,24993	188,8101	181,3936	0,68162	0,15526	0,25502	0,26516	0,47846	25,83716	1,42575	1,23147
00002489_J_500_palm_02	84	0,45232	0,13207	33	56	0,55357	0,67857	144,43803	0,83260	0,12965	172,3419	168,7057	0,80312	0,16612	0,29108	0,26975	0,72406	82,54341	1,03670	0,33118
00002494_J_500_palm_04	40	0,43841	0,20271	50	75	0,40000	0,01333	170,75412	0,67911	0,21474	199,5484	196,4742	0,49006	0,18419	0,26658	0,18443	0,39929	24,35703	1,20393	0,81394
00002494_J_500_palm_10	13	0,52558	0,29840	78	100	0,44000	0,08000	141,30249	0,69939	0,18428	181,0809	169,7650	0,59730	0,20065	0,21036	0,09981	0,45884	31,20123	1,22447	1,00043
00002494_S_500_slap_03	75	0,38161	0,13554	34	56	0,41071	0,14285	170,49641	0,76361	0,12955	194,5903	187,8383	0,68154	0,15594	0,32499	0,29393	0,53225	50,56414	1,15999	0,58891
00002495_J_500_palm_03	86	0,47820	0,18519	24	59	0,64406	0,25423	182,55675	0,80111	0,19112	203,4311	199,5541	0,70142	0,18321	0,36473	0,35267	0,58568	78,48236	1,13512	1,02644

Table A.1 *(continued)*

Identifier	$O_{NFIQ2\ v2.3.0}$	q^μ_{FDA}	q^σ_{FDA}	q^{COM}_{MIN}	q^{CNT}_{MIN}	q^{MU}_{MIN}	q^{OCL}_{MIN}	q^μ_{AREA}	q^μ_{LCL}	q^σ_{LCL}	q_{MMB}	q_{MU}	q^μ_{OCL}	q^σ_{OCL}	q^μ_{OFL}	q^σ_{OFL}	q^{REL}_{COH}	q^{sum}_{COH}	q^μ_{RVU}	q^σ_{RVU}
00002495_S_500_slap_08	83	0,46179	0,16234	24	52	0,75000	0,23076	182,77830	0,76287	0,23545	201,5593	198,2629	0,65630	0,20598	0,30970	0,32627	0,53312	59,17648	1,13182	0,64084
00002497_N_500_palm_08	16	0,49304	0,34219	47	50	0,50000	0,00000	223,29629	0,49523	0,33384	241,2249	241,2835	0,37130	0,23069	0,14697	0,07717	0,35444	12,05122	1,25546	0,82725
00002497_N_500_palm_09	0	0,56000	0,34077	169	219	0,47488	0,00000	195,70155	0,54530	0,29471	227,0198	224,5644	0,41638	0,20429	0,42953	0,23779	0,35540	17,77020	1,36079	1,37437
00002502_Q_500_palm_05	29	0,48832	0,26915	54	61	0,77049	0,06557	113,60927	0,73135	0,12532	149,4669	139,1367	0,59346	0,19895	0,37408	0,27058	0,45290	33,51516	1,43200	1,43022
00002504_N_500_palm_03	83	0,44128	0,16722	42	113	0,38938	0,31858	153,28360	0,69560	0,29662	185,8852	183,6091	0,73863	0,19557	0,32904	0,31113	0,65130	74,90033	1,17871	0,67056
00002504_S_500_slap_06	93	0,44950	0,16859	36	87	0,58658	0,24137	155,71579	0,77363	0,16211	176,2892	175,0218	0,68387	0,18236	0,34230	0,30628	0,54632	89,59673	1,15977	0,87416
00002505_N_500_palm_10	12	0,57333	0,31513	30	44	0,43481	0,18181	147,60927	0,66681	0,25460	187,7016	179,7347	0,59771	0,20185	0,15279	0,24003	0,46019	34,05472	1,27926	1,07343
00002514_Q_500_palm_03	72	0,43407	0,15839	29	40	0,45000	0,00000	170,45351	0,79458	0,16188	198,3571	193,2994	0,73227	0,13514	0,30440	0,29443	0,59187	37,88015	1,12803	0,47172
00002516_S_500_slap_09	48	0,44698	0,25081	70	123	0,63414	0,06504	142,75625	0,75421	0,15906	168,4901	162,8628	0,66369	0,17167	0,20186	0,21585	0,50026	49,52576	1,28680	0,96569
00002521_Q_500_palm_10	13	0,45471	0,27447	107	244	0,62295	0,01229	150,56760	0,60043	0,27207	171,3819	166,0930	0,53849	0,17251	0,22846	0,21640	0,38513	45,83083	1,30934	1,23989
00002523_J_500_palm_03	70	0,47002	0,21026	36	54	0,61111	0,01851	206,48448	0,74774	0,15394	222,1027	218,3158	0,59699	0,19561	0,32496	0,27386	0,44682	33,06466	1,14953	0,75956
00002523_J_500_palm_05	8	0,46941	0,29825	103	123	0,47967	0,00000	189,25872	0,59874	0,27243	212,3879	208,0669	0,47163	0,19327	0,30969	0,24281	0,37379	19,81125	1,45088	1,34989
00002523_S_500_slap_04	48	0,41938	0,21120	78	113	0,70796	0,02654	180,19840	0,74398	0,14263	205,0201	196,0977	0,62041	0,14974	0,38895	0,27383	0,47453	40,33516	1,21783	0,85807
00002523_S_500_slap_05	19	0,43000	0,25078	122	145	0,72413	0,00689	191,23440	0,63127	0,25967	210,1260	206,0959	0,60029	0,18497	0,19461	0,21160	0,43883	28,96334	1,37342	1,42120
00002528_N_500_palm_05	59	0,43420	0,22570	40	74	0,45945	0,31081	127,23412	0,74614	0,19186	161,3593	153,1599	0,73221	0,18568	0,29203	0,29057	0,62165	66,51666	1,18349	0,71708
00002531_Q_500_palm_09	35	0,47681	0,27513	70	94	0,38297	0,13829	130,16226	0,73514	0,21821	154,8473	151,9704	0,74183	0,18619	0,33895	0,30691	0,56829	46,03169	1,23192	1,05229
00002533_N_500_palm_10	27	0,45695	0,26658	136	202	0,61386	0,03465	96,38731	0,66134	0,25380	137,9797	132,9817	0,63563	0,20287	0,35011	0,28141	0,49877	47,38394	1,25607	0,99186
00002533_Q_500_palm_09	50	0,41828	0,21713	97	164	0,61585	0,16463	92,49101	0,72409	0,20861	125,6309	125,0877	0,71744	0,22106	0,21350	0,25429	0,59223	63,96182	1,18954	0,88829
00002533_S_500_slap_08	58	0,45642	0,24179	52	58	0,44827	0,24137	132,45085	0,68872	0,28096	166,9048	156,8935	0,80731	0,13636	0,43772	0,28369	0,67054	46,93791	1,07420	0,57807
00002534_N_500_palm_05	54	0,41306	0,20576	34	43	0,34883	0,23255	132,04778	0,73331	0,19653	175,3678	160,7387	0,68702	0,13300	0,33668	0,28362	0,54979	37,93554	1,14345	0,59991
00002544_S_500_slap_03	88	0,43976	0,13352	30	75	0,52000	0,25333	156,18909	0,79820	0,13941	177,4049	173,2623	0,68493	0,16064	0,22237	0,25829	0,54666	75,43962	1,10302	0,58680

Table A.1 *(continued)*

Identifier	$Q_{NFIQ2\ v2.3.0}$	q_{FDA}^{μ}	q_{FDA}^{σ}	q_{MIN}^{COM}	q_{MIN}^{CNT}	q_{MIN}^{MU}	q_{MIN}^{OCL}	q_{AREA}^{μ}	q_{LCL}^{μ}	q_{LCL}^{σ}	q_{MMB}	q_{MU}	q_{OCL}^{μ}	q_{OCL}^{σ}	q_{OFL}^{μ}	q_{OFL}^{σ}	q_{COH}^{REL}	q_{COH}^{sum}	q_{RVU}^{μ}	q_{RVU}^{σ}
00002544_S_500_slap_08	84	0,472 54	0,183 57	22	88	0,568 18	0,125 00	170,529 92	0,777 08	0,199 78	190,233 5	187,583 0	0,689 55	0,159 03	0,188 96	0,260 12	0,573 46	74,550 18	1,095 30	0,607 53
00002547_N_500_palm_08	70	0,379 34	0,130 75	38	65	0,553 84	0,230 76	124,879 03	0,779 59	0,164 25	152,458 7	143,163 2	0,720 09	0,124 95	0,229 19	0,210 60	0,552 19	55,219 12	1,130 37	0,762 90
00002547_Q_500_palm_03	73	0,426 58	0,166 52	40	70	0,314 28	0,114 28	134,742 16	0,782 36	0,132 08	167,712 4	157,401 2	0,680 57	0,131 48	0,347 12	0,286 63	0,517 04	52,221 01	1,207 49	0,701 55
00002547_S_500_slap_04	65	0,413 48	0,213 13	35	62	0,193 54	0,096 77	130,824 92	0,767 75	0,143 53	177,322 8	172,814 1	0,676 90	0,122 71	0,307 71	0,273 92	0,511 21	44,475 34	1,208 16	0,821 18
00002551_S_500_slap_10	48	0,391 81	0,220 87	66	74	0,256 75	0,081 08	184,406 87	0,424 31	0,359 58	219,598 3	213,267 6	0,569 34	0,215 16	0,266 55	0,172 63	0,535 08	22,473 68	1,266 72	1,062 71
00002554_J_500_palm_08	17	0,468 78	0,295 90	73	103	0,271 84	0,000 00	198,092 11	0,603 31	0,277 49	221,988 7	218,398 0	0,511 86	0,215 27	0,358 22	0,372 10	0,431 81	32,817 59	1,268 96	0,912 66
00002554_S_500_slap_07	26	0,409 02	0,241 16	158	204	0,549 02	0,000 00	210,641 46	0,509 27	0,320 81	223,541 1	220,343 5	0,480 48	0,152 37	0,255 49	0,276 43	0,337 65	29,038 13	1,293 17	1,013 13
00002555_S_500_slap_08	64	0,415 57	0,193 15	40	68	0,352 94	0,500 00	107,037 41	0,709 29	0,260 55	151,798 4	139,742 8	0,777 89	0,175 28	0,289 39	0,297 36	0,678 33	65,119 69	1,162 13	0,608 21
00002559_S_500_slap_05	10	0,459 95	0,296 12	129	231	0,411 25	0,038 96	082,564 94	0,564 06	0,301 49	207,426 7	203,253 0	0,583 49	0,196 00	0,284 32	0,307 47	0,425 29	43,380 22	1,281 46	1,054 81
00002559_S_500_slap_07	62	0,407 88	0,195 10	36	100	0,330 00	0,030 00	178,414 24	0,634 98	0,286 16	203,966 7	202,657 0	0,644 56	0,113 31	0,187 96	0,215 18	0,498 74	50,872 35	1,140 76	0,806 73
00002559_S_500_slap_09	62	0,392 13	0,184 44	38	87	0,436 78	0,229 88	152,237 17	0,705 20	0,221 31	180,247 2	177,379 1	0,709 71	0,165 67	0,190 11	0,262 40	0,567 66	70,389 97	1,105 64	0,665 85
00002560_N_500_palm_10	18	0,431 04	0,211 33	24	26	0,153 84	0,000 00	162,270 37	0,706 82	0,216 01	197,212 7	189,381 4	0,598 05	0,193 36	0,233 70	0,242 62	0,476 07	26,659 94	1,137 10	0,498 57
00002564_S_500_slap_09	4	0,489 67	0,330 58	176	255	0,376 47	0,003 92	171,143 08	0,588 26	0,257 11	203,048 5	188,509 5	0,421 76	0,179 20	0,456 76	0,333 11	0,291 16	24,166 99	1,247 40	1,109 07
00002568_J_500_palm_04	22	0,434 91	0,256 18	122	172	0,319 76	0,023 25	128,242 52	0,598 36	0,298 01	155,919 9	147,305 5	0,557 74	0,237 56	0,459 36	0,345 51	0,442 05	38,458 51	1,143 34	0,901 32
00002568_J_500_palm_10	31	0,447 69	0,268 36	137	166	0,566 26	0,030 12	170,068 61	0,491 40	0,363 61	196,816 6	188,430 1	0,638 57	0,199 44	0,228 57	0,279 24	0,466 35	33,577 44	1,225 97	0,973 13
00002569_N_500_palm_08	20	0,415 30	0,252 48	104	191	0,633 50	0,000 00	190,511 34	0,659 81	0,235 24	203,251 1	199,495 5	0,553 28	0,172 94	0,508 64	0,396 08	0,400 74	42,078 46	1,321 08	1,091 03
00002569_N_500_palm_09	9	0,440 78	0,290 86	144	255	0,423 52	0,000 00	186,023 54	0,625 58	0,261 01	204,186 4	201,656 9	0,511 96	0,149 38	0,596 20	0,360 95	0,343 76	38,502 17	1,226 07	0,965 44
00002569_S_500_slap_01	74	0,398 07	0,149 06	39	90	0,744 44	0,144 44	168,370 22	0,771 58	0,174 10	185,654 4	183,246 9	0,740 75	0,106 57	0,378 06	0,359 30	0,590 32	93,270 56	1,110 80	0,645 70
00002569_S_500_slap_03	37	0,393 87	0,192 55	82	151	0,721 85	0,000 00	161,956 17	0,749 00	0,164 75	181,240 1	178,696 9	0,601 18	0,173 51	0,364 37	0,349 62	0,442 67	52,677 80	1,229 05	0,994 02
00002569_S_500_slap_08	16	0,436 41	0,282 13	88	208	0,620 19	0,014 42	192,376 69	0,649 49	0,244 95	204,325 4	200,511 8	0,617 74	0,168 38	0,364 69	0,229 46	0,442 32	49,540 55	1,300 73	1,069 70
00002571_S_500_slap_07	88	0,417 69	0,118 47	25	52	0,596 15	0,365 38	200,542 26	0,790 14	0,189 81	216,190 0	213,754 1	0,747 92	0,150 67	0,261 25	0,265 53	0,645 16	67,096 79	1,096 38	0,449 48

Table A.1 *(continued)*

Identifier	$O_{\text{NFIQ2 v2.3.0}}$	q^{μ}_{FDA}	q^{σ}_{FDA}	q^{COM}_{MIN}	q^{CNT}_{MIN}	q^{MU}_{MIN}	q^{OCL}_{MIN}	q^{μ}_{AREA}	q^{μ}_{LCL}	q^{σ}_{LCL}	q_{MMB}	q_{MU}	q^{μ}_{OCL}	q^{σ}_{OCL}	q^{μ}_{OFL}	q^{σ}_{OFL}	q^{REL}_{COH}	q^{sum}_{COH}	q^{μ}_{RVU}	q^{σ}_{RVU}
00002571_S_500_slap_10	81	0,446 84	0,174 85	33	51	0,352 94	0,490 19	172,018 64	0,763 70	0,258 61	202,623 7	198,973 0	0,781 16	0,154 28	0,235 21	0,237 92	0,709 47	64,562 31	1,136 56	0,414 46
00002573_Q_500_palm_03	67	0,438 67	0,175 80	40	80	0,425 00	0,362 50	128,830 08	0,780 10	0,139 89	158,581 5	152,357 4	0,752 13	0,171 58	0,392 77	0,361 61	0,620 24	64,504 94	1,135 98	0,723 20
00002573_Q_500_palm_04	58	0,427 13	0,200 52	74	127	0,511 81	0,228 34	138,904 50	0,697 12	0,238 80	171,260 4	164,243 6	0,711 48	0,186 28	0,294 42	0,320 25	0,573 10	57,310 45	1,118 72	0,719 35
00002574_S_500_slap_06	86	0,443 17	0,176 27	30	115	0,321 73	0,452 17	135,760 49	0,777 14	0,207 31	171,898 1	163,897 2	0,775 58	0,212 83	0,281 13	0,315 57	0,679 14	101,871 37	1,106 95	0,633 50
00002577_N_500_palm_09	40	0,489 44	0,291 30	54	109	0,192 66	0,110 09	120,840 03	0,679 22	0,243 44	174,159 4	165,874 9	0,615 06	0,215 26	0,297 86	0,366 08	0,574 58	49,414 53	1,213 19	1,183 01
00002578_N_500_palm_04	62	0,427 89	0,201 43	45	97	0,670	0,061 85	171,828 29	0,692 10	0,233 02	195,200 9	188,714 5	0,595 01	0,148 05	0,353 36	0,302 39	0,433 05	42,872 32	1,089 56	0,656 59
00002579_J_500_palm_05	34	0,462 58	0,261 97	114	154	0,461 03	0,038 96	141,967 00	0,689 97	0,224 45	176,895 2	171,717 7	0,648 37	0,174 18	0,257 50	0,222 75	0,532 88	51,156 79	1,180 42	0,880 77
00002579_J_500_palm_08	89	0,457 53	0,177 57	29	64	0,625 00	0,637 50	160,286 41	0,808 18	0,149 78	175,976 3	173,456 4	0,806 67	0,148 04	0,343 51	0,329 75	0,689 48	84,806 84	1,176 48	0,535 33
00002581_Q_500_palm_10	20	0,471 33	0,292 89	157	197	0,812 18	0,000 00	079,660 15	0,572 97	0,317 66	205,390 2	202,017 6	0,587 95	0,167 27	0,367 38	0,301 55	0,430 10	35,698 79	1,169 70	0,756 40
00002581_S_500_slap_08	66	0,424 56	0,191 26	42	70	0,628 57	0,071 42	176,440 46	0,660 88	0,271 27	193,879 5	187,676 6	0,691 12	0,120 01	0,394 99	0,314 28	0,533 26	55,459 52	1,146 24	0,637 09
00002584_J_500_palm_09	3	0,478 23	0,313 57	146	233	0,721 03	0,000 00	236,679 01	0,526 40	0,321 38	239,651 5	239,446 8	0,463 93	0,178 66	0,368 70	0,327 45	0,321 61	39,236 43	1,334 24	1,250 81
00002586_S_500_slap_01	90	0,453 63	0,146 30	37	92	0,597 82	0,195 65	158,869 86	0,794 97	0,142 74	182,560 7	179,000 8	0,632 50	0,191 30	0,332 67	0,308 05	0,469 83	81,281 52	1,138 60	0,620 04
00002588_J_500_palm_07	51	0,418 65	0,216 25	53	71	0,577 46	0,084 50	184,905 71	0,690 43	0,229 87	204,940 3	199,287 9	0,654 15	0,179 80	0,215 30	0,186 74	0,502 59	32,668 48	0,968 04	0,476 38
00002591_S_500_slap_01	79	0,390 19	0,116 93	35	70	0,642 85	0,785 71	110,583 60	0,825 73	0,104 15	148,217 7	135,880	0,862 73	0,110 29	0,409 75	0,304 70	0,723 41	81,746 25	1,152 30	0,512 47
00002593_Q_500_palm_05	31	0,388 18	0,190 85	110	155	0,696 77	0,000 00	195,613 18	0,615 53	0,257 58	210,744 0	209,910 8	0,515 55	0,123 36	0,362 97	0,290 28	0,354 87	28,035 45	1,301 14	1,081 32
00002610_S_500_slap_06	94	0,422 72	0,138 42	33	150	0,553 33	0,106 66	172,132 19	0,760 66	0,201 10	194,916 2	188,477 5	0,682 93	0,224 00	0,265 63	0,291 62	0,481 16	89,977 89	1,122 61	0,604 80
00002616_Q_500_palm_07	13	0,426 79	0,257 80	102	154	0,233 76	0,000 00	169,416 41	0,640 58	0,237 65	193,217 8	191,084 5	0,495 09	0,152 69	0,265 46	0,272 19	0,342 89	26,745 78	1,242 22	0,910 13
00002624_Q_500_palm_07	75	0,424 60	0,128 55	35	63	0,587 30	0,047 61	188,285 25	0,753 10	0,208 58	203,019 6	201,475 4	0,661 21	0,146 03	0,205 99	0,216 80	0,495 25	47,049 49	1,122 14	0,431 17
00002626_S_500_slap_04	65	0,460 99	0,162 48	21	39	0,435 89	0,153 84	174,368 40	0,812 75	0,135 35	195,437 3	193,209 1	0,718 56	0,156 45	0,225 65	0,284 88	0,547 61	55,856 37	1,152 70	0,775 88
00002633_S_500_slap_09	51	0,434 82	0,221 73	56	110	0,500 00	0,309 09	131,309 52	0,625 01	0,323 46	160,080 5	152,347 1	0,759 74	0,142 47	0,225 61	0,223 96	0,613 54	62,581 28	1,161 98	0,719 67
00002633_S_500_slap_10	44	0,405 13	0,247 55	94	135	0,511 11	0,044 44	206,836 05	0,533 72	0,314 15	220,279 1	218,582 0	0,521 03	0,215 22	0,248 16	0,229 63	0,406 02	28,422 06	1,268 76	1,222 56

Table A.1 *(continued)*

Identifier	$Q_{NFIQ2\,v2.3.0}$	q_{FDA}^{μ}	q_{FDA}^{σ}	q_{MIN}^{COM}	q_{MIN}^{CNT}	q_{MIN}^{MU}	q_{MIN}^{OCL}	q_{AREA}^{μ}	q_{LCL}^{μ}	q_{LCL}^{σ}	q_{MMB}	q_{MU}	q_{OCL}^{μ}	q_{OCL}^{σ}	q_{OFL}^{μ}	q_{OFL}^{σ}	q_{COH}^{REL}	q_{COH}^{sum}	q_{RVU}^{μ}	q_{RVU}^{σ}
00002636_S_500_slap_07	67	0,39516	0,14123	36	70	0,31428	0,10000	184,93770	0,69179	0,26260	208,8194	203,1632	0,60790	0,22728	0,49770	0,37665	0,51376	42,12900	1,12501	0,66882
00002636_S_500_slap_09	56	0,41821	0,24652	53	101	0,57425	0,06930	204,92751	0,47330	0,35757	220,7890	218,4580	0,61140	0,20621	0,27660	0,27547	0,51034	42,35818	1,22330	0,94506
00002640_Q_500_palm_04	9	0,46036	0,29868	108	164	0,12195	0,00000	142,96940	0,50757	0,30571	186,5486	180,4493	0,41307	0,17059	0,42234	0,25526	0,29581	18,34054	1,31227	0,96076
00002641_I_500_palm_04	47	0,48096	0,20625	70	98	0,36734	0,11224	137,50112	0,74725	0,19805	167,6775	163,0938	0,66855	0,19347	0,38350	0,31217	0,54390	45,14393	1,11200	0,56303
00002641_S_500_slap_03	71	0,43624	0,17490	43	57	0,57894	0,52631	148,08420	0,72050	0,27223	175,3182	170,6682	0,85434	0,08958	0,31157	0,27425	0,74880	54,66249	1,11371	0,72277
00002644_S_500_slap_01	80	0,43884	0,17334	28	74	0,36486	0,66216	101,39070	0,82368	0,13102	145,9518	136,9262	0,84692	0,12456	0,30048	0,30057	0,72612	121,26294	1,16163	0,53415
00002645_S_500_slap_01	96	0,44092	0,14295	38	88	0,65909	0,21590	164,43903	0,78940	0,15527	187,0670	183,3706	0,66581	0,20100	0,36692	0,32531	0,51282	74,87301	1,03730	0,48247
00002645_S_500_slap_10	25	0,46083	0,25319	67	78	0,19230	0,06410	162,51241	0,63581	0,27309	193,3860	188,1090	0,57317	0,19127	0,36073	0,24414	0,44752	27,29906	1,31704	1,24072
00002649_Q_500_palm_09	35	0,47326	0,27434	67	154	0,60389	0,12987	116,60116	0,55641	0,34260	142,3163	136,4620	0,66539	0,26540	0,30814	0,37502	0,53637	71,33843	1,19068	0,78405
00002650_S_500_slap_07	65	0,39906	0,13341	36	73	0,30137	0,24657	183,81048	0,73836	0,24732	207,7897	202,2469	0,68799	0,25272	0,43097	0,34833	0,62918	59,77218	1,11713	0,63273
00002650_S_500_slap_08	64	0,39198	0,14537	74	141	0,29787	0,12766	195,69012	0,67297	0,30553	212,4925	208,8935	0,66869	0,23196	0,33165	0,28499	0,58268	62,92952	1,18314	0,87125
blank_fd249	NA	NA	NA	NA	NA	NA	NA	NA	NA	NA	NA	NA	NA	NA	NA	NA	NA	NA	NA	NA
solid_0_500x500	NA	NA	NA	NA	NA	NA	NA	NA	NA	NA	NA	NA	NA	NA	NA	NA	NA	NA	NA	NA
solid_0_800x1000	NA	NA	NA	NA	NA	NA	NA	NA	NA	NA	NA	NA	NA	NA	NA	NA	NA	NA	NA	NA
solid_0_800x1001	NA	NA	NA	NA	NA	NA	NA	NA	NA	NA	NA	NA	NA	NA	NA	NA	NA	NA	NA	NA
solid_0_801x1000	NA	NA	NA	NA	NA	NA	NA	NA	NA	NA	NA	NA	NA	NA	NA	NA	NA	NA	NA	NA
solid_250_500x500	NA	NA	NA	NA	NA	NA	NA	NA	NA	NA	NA	NA	NA	NA	NA	NA	NA	NA	NA	NA
solid_251_500x500	NA	NA	NA	NA	NA	NA	NA	NA	NA	NA	NA	NA	NA	NA	NA	NA	NA	NA	NA	NA
solid_255_500x500	NA	NA	NA	NA	NA	NA	NA	NA	NA	NA	NA	NA	NA	NA	NA	NA	NA	NA	NA	NA

Key

NA	value not computed (not applicable)
$Q_{NFIQ2\,v2.3.0}$	unified quality score
q_{FDA}^{μ}	mean of local frequency domain analysis
q_{FDA}^{σ}	standard deviation of local frequency domain analysis
q_{MIN}^{COM}	minutiae count in centre of mass
q_{MMB}	MMB
q_{MU}	MU
q_{OCL}^{μ}	mean of local orientation certainty level
q_{OCL}^{σ}	standard deviation of local orientation certainty level
q_{OFL}^{μ}	mean of local orientation flow

Table A.1 *(continued)*

Identifier	$O_{NFIQ2\,v2.3.0}$	q_{FDA}^{μ}	q_{FDA}^{σ}	q_{MIN}^{COM}	q_{MIN}^{CNT}	q_{MIN}^{MU}	q_{MIN}^{OCL}	q_{AREA}^{μ}	q_{LCL}^{μ}	q_{LCL}^{σ}	q_{MMB}	q_{MU}	q_{OCL}^{μ}	q_{OCL}^{σ}	q_{OFL}^{μ}	q_{OFL}^{σ}	q_{COH}^{REL}	q_{COH}^{sum}	q_{RVU}^{μ}	q_{RVU}^{σ}
q_{MIN}^{CNT}	minutiae count									q_{OFL}^{σ}	standard deviation of local orientation flow									
q_{MIN}^{MU}	minutiae quality based in image mean									q_{COH}^{sum}	region of interest orientation map coherence sum									
q_{MIN}^{OCL}	minutiae quality based on orientation certainty level									q_{COH}^{REL}	region of interest relative orientation map coherence sum									
q_{AREA}^{μ}	region of interest image mean									q_{RVU}^{μ}	mean of local ridge valley uniformity									
q_{LCL}^{μ}	mean of local clarity									q_{RVU}^{σ}	standard deviation of local ridge valley uniformity									
q_{LCL}^{σ}	standard deviation of local clarity																			

Table A.2 — Target quality component values mapped 0-100 for conformance test set

Identifier	Q^{μ}_{FDA}	Q^{σ}_{FDA}	Q^{COM}_{MIN}	Q^{CNT}_{MIN}	Q^{MU}_{MIN}	Q^{OCL}_{MIN}	Q^{μ}_{AREA}	Q^{μ}_{LCL}	Q^{σ}_{LCL}	Q_{MMB}	Q_{MU}	Q^{μ}_{OCL}	Q^{σ}_{OCL}	Q^{μ}_{OFL}	Q^{σ}_{OFL}	Q^{REL}_{COH}	Q^{sum}_{COH}	Q^{μ}_{RVU}	Q^{σ}_{RVU}
00001052_plain_500_10	NA	NA	NA	NA	NA	NA	NA	NA	NA	NA	NA	NA	NA	NA	NA	NA	NA	NA	NA
00001057_plain_500_03	46	20	32	55	33	71	57	81	17	65	64	83	15	17	30	70	2	56	41
00001308_plain_500_08	48	20	16	44	43	59	64	81	21	71	71	78	15	11	22	69	2	57	33
00001428_plain_500_07	56	26	31	88	26	29	66	76	24	73	73	75	17	19	35	62	2	57	43
00001610_plain_500_10	64	33	100	100	42	3	63	62	28	71	70	60	22	15	24	47	1	65	52
00001655_plain_500_04	47	26	89	100	13	2	62	73	22	72	72	64	17	17	35	53	2	60	47
00001665_plain_500_08	59	34	76	100	32	0	64	64	27	72	70	55	17	18	35	38	1	65	55
00001723_plain_500_05	56	29	30	57	21	46	58	63	35	68	67	74	18	15	29	66	1	60	51
00001880_plain_500_10	68	34	100	100	7	2	50	55	33	65	63	59	20	23	29	44	1	75	71
00002302_N_500_palm_10	54	29	79	95	50	0	66	64	24	77	74	49	17	19	28	35	0	55	38
00002302_N_500_palm_10-core	38	19	42	42	43	0	59	65	20	65	62	42	17	19	3	31	0	60	55
00002304_R_500_slap_01	43	17	36	100	33	39	67	70	29	80	79	73	20	18	35	66	2	54	29
00002304_R_500_slap_08	43	22	61	100	45	3	68	70	21	78	77	56	20	19	48	44	0	57	52
00002310_R_500_slap_05	41	24	63	100	47	10	55	67	25	69	66	66	19	16	25	50	1	54	31
00002314_R_500_slap_01	45	17	31	65	54	6	72	75	22	81	80	62	15	20	38	49	2	57	35
00002315_R_500_slap_05	51	32	100	100	60	0	65	60	26	75	72	45	21	22	29	32	0	62	47
00002315_R_500_slap_06	43	19	53	100	44	15	61	76	17	72	69	72	16	19	36	58	3	55	30
00002317_R_500_slap_01	45	13	31	100	73	26	62	81	14	73	71	70	16	19	34	55	3	54	30
00002319_R_500_slap_04	42	16	57	83	58	2	75	55	37	80	80	60	14	26	44	42	1	53	30
00002319_R_500_slap_09	42	16	37	92	65	0	75	60	31	84	83	53	15	24	37	40	1	53	27
00002319_R_500_slap_10	46	18	25	44	73	2	72	75	21	82	81	63	14	8	17	50	1	55	24
00002320_R_500_slap_06	43	25	19	100	30	12	57	72	18	65	64	65	17	16	31	49	2	63	49
00002320_R_500_slap_08	46	29	100	100	37	0	62	61	26	67	67	55	18	20	31	40	1	69	65
00002321_R_500_slap_07	45	28	100	100	57	3	74	64	25	82	79	53	20	21	31	37	1	66	55

Table A.2 *(continued)*

Identifier	Q^{μ}_{FDA}	Q^{σ}_{FDA}	Q^{COM}_{MIN}	Q^{CNT}_{MIN}	Q^{MU}_{MIN}	Q^{OCL}_{MIN}	Q^{μ}_{AREA}	Q^{μ}_{LCL}	Q^{σ}_{LCL}	Q_{MMB}	Q_{MU}	Q^{μ}_{OCL}	Q^{σ}_{OCL}	Q^{μ}_{OFL}	Q^{σ}_{OFL}	Q^{REL}_{COH}	Q^{sum}_{COH}	Q^{μ}_{RVU}	Q^{σ}_{RVU}
00002325_R_500_slap_04	43	25	72	100	23	2	54	68	23	65	64	58	15	21	33	42	1	54	45
00002325_R_500_slap_08	45	27	67	100	17	7	51	63	26	65	63	59	19	19	30	44	1	69	66
00002326_R_500_slap_02	43	17	34	100	41	7	68	78	14	77	76	71	16	14	26	54	2	59	35
00002326_R_500_slap_05	46	30	100	100	42	0	72	58	30	80	80	54	18	21	34	38	1	64	49
00002330_R_500_slap_04	41	20	67	100	65	9	64	62	30	74	72	62	17	16	32	46	1	59	33
00002334_R_500_slap_05	40	24	80	89	53	12	57	64	28	67	65	73	13	13	24	55	1	61	43
00002334_R_500_slap_07	42	17	46	82	64	24	64	69	28	76	73	74	17	19	31	58	1	55	28
00002340_R_500_slap_08	39	25	98	100	58	2	59	49	33	82	82	59	17	21	35	42	1	61	41
00002342_R_500_slap_05	51	34	100	100	46	0	64	54	31	74	72	58	14	10	19	41	1	72	61
00002342_R_500_slap_09	43	29	79	100	38	0	64	64	25	75	74	53	20	10	20	42	1	65	56
00002349_N_500_palm_05	44	26	63	100	50	0	41	75	14	58	56	61	18	10	20	45	1	60	41
00002349_R_500_slap_07	47	28	99	100	52	1	52	68	22	65	63	57	15	19	31	43	1	63	52
00002352_R_500_slap_01	47	17	24	99	77	42	59	78	23	72	68	80	13	17	35	68	3	55	33
00002352_R_500_slap_10	39	21	45	78	72	6	73	69	21	81	79	60	15	15	28	45	1	67	47
00002353_N_500_palm_10	46	27	79	100	42	42	58	40	39	74	71	75	20	17	31	64	1	59	37
00002353_R_500_slap_06	41	18	60	100	30	58	50	50	38	65	63	83	14	14	30	76	3	54	31
00002353_R_500_slap_10	44	27	88	100	55	27	72	33	38	84	82	68	15	14	26	53	1	60	55
00002356_N_500_palm_05	42	17	52	89	34	2	51	81	5	63	62	70	12	21	37	53	1	69	66
00002357_R_500_slap_02	43	16	31	53	55	30	56	80	13	66	64	76	13	20	27	61	1	54	31
00002357_R_500_slap_04	36	14	63	96	83	24	46	75	19	57	55	77	14	16	27	61	2	58	30